R90-917810-5

A Study of the Critical Factors Controlling the Synthesis of Ceramic Matrix Composites from Preceramic Polymers

J.R. Strife and J.P. Wesson
United Technologies Research Center
East Hartford, CT 06108
and
H.H. Streckert
GA Technologies Inc.
San Diego, CA 92138

Sponsored by
Defense Advanced Research Projects Agency
DARPA Order No. 6153

Monitored by AFOSR Under Contract No. F49620-87-C-0093

15 December 1990

Final Technical Report
for period 1 Oct 1987 through 15 Nov 1990

UNITED TECHNOLOGIES RESEARCH CENTER
East Hartford, Connecticut 06108

REPORT DOCUMENTATION PAGE

Form Approved
OMB No 0704-0188

1. AGENCY USE ONLY (Leave blank)	2. REPORT DATE	3. REPORT TYPE AND DATES COVERED
	15 December 1990	Final 1 Oct 1987 - 15 Nov 1990

4. TITLE AND SUBTITLE

A STUDY OF THE CRITICAL FACTORS CONTROLLING THE SYNTHESIS OF CERAMIC MATRIX COMPOSITES FROM PRECERAMIC POLYMERS

5. FUNDING NUMBERS

C - F49620-87-C-0093
PE - 61102F
PR - 9999
TA - 99

6. AUTHOR(S)

J. R. Strife(1), J. P. Wesson(1), and H. H. Streckert(2)

7. PERFORMING ORGANIZATION NAME(S) AND ADDRESS(ES)

(1)United Technologies Research Center
East Hartford, CT 06108
(2) GA Technologies, Inc.
San Diego, CA 92138

8. PERFORMING ORGANIZATION REPORT NUMBER

R90-917810-5

9. SPONSORING MONITORING AGENCY NAME(S) AND ADDRESS(ES)

Dr. Liselotte J. Schioler
Air Force Office of Scientific Research
Bolling Air Force Base
Washington, DC 20332

10. SPONSORING MONITORING AGENCY REPORT NUMBER

3316/A2

11. SUPPLEMENTARY NOTES

12a. DISTRIBUTION AVAILABILITY STATEMENT

Unlimited

12b. DISTRIBUTION CODE

13. ABSTRACT (Maximum 200 words)

In this three year program, vinylmethylsilane co-polymers which were processable at ambient pressure were studied as precursors for silicon carbide matrix composites. Using measurements of curing characteristics, rheological properties, and pyrolysis kinetics, fabrication cycles for processing carbon fabric reinforced composites were identified. Composites exhibiting a range of useful mechanical properties were demonstrated. The primary shortcomings of a commercially available vinylmethylsilane polymer used in composite fabrication were identified as extreme sensitivity to oxygen contamination during processing and excess carbon in the pyrolyzed products. Analytical methods showed that 900°C pyrolysis products were amorphous ceramics consisting primarily of Si-O-C complexes. The amorphous ceramic was unstable above 1200°C where CO and CO_2 release initiated. Ceramic products converted at 1440°C showed increases in β-SiC and SiO_2 content at the expense of Si-O-C content. Polymer modifications were pursued to improve the converted ceramic thermal stability and stoichiometry. Novel methylvinylsilanes with reactive endgroups exhibited significantly reduced oxygen sensitivity and high ceramic convertibility. The converted ceramic from this polymer showed SiC, SiO_2, and Si-O-C complexes as primary microstructural components, and possessed remarkable thermal stability at temperatures up to 1500°C.

14. SUBJECT TERMS

C-SiC composites
polymer precursor
vinylmethylsilane
end-blocked vinylmethylsilane

15. NUMBER OF PAGES
49

16. PRICE CODE

17. SECURITY CLASSIFICATION OF REPORT	18. SECURITY CLASSIFICATION OF THIS PAGE	19. SECURITY CLASSIFICATION OF ABSTRACT	20. LIMITATION OF ABSTRACT
Unclassified	Unclassified	Unclassified	UL

UNITED
TECHNOLOGIES
RESEARCH
CENTER
East Hartford, Connecticut 06108

R90-917810-5

A Study of the Critical Factors Controlling the Synthesis of Ceramic Matrix Composites from Preceramic Polymers

by

J.R. Strife, J.P. Wesson, and H.H. Streckert

Final Technical Report
DARPA Order No. 6153
AFOSR Contract F49620-87-C-0093

APPROVED BY K. M. Prewo

K. M. Prewo, Manager of
Materials Sciences

DATE 12/15/90

TABLE OF CONTENTS

INTRODUCTION

Current DoD technology thrusts such as the Integrated High Performance Turbine Engine Technology Program and the National Aerospace Plane Program depend on the development of high temperature low density materials. Fiber reinforced ceramics are projected to play a major role because of their high temperature capacity and superior mechanical properties on a density normalized basis at elevated temperature. Processing of fiber reinforced ceramics has been pursued primarily by hot pressing tape materials or by the chemical vapor infiltration of fibrous preforms. More recently, the conversion of preceramic polymers as a matrix synthesis process is being considered. This approach offers several advantages relative to the other processes for the fabrication of ceramic composites. First, a range of useful composite matrices can be conceived based on carbide, oxide, and nitride precursors. Second, by using a polymer approach, fillers and other additives may be easily incorporated into the composite enabling the synthesis of multi-phase compositions. Third, reproducible matrix characteristics can be anticipated by controlling polymer chemistry and composite fabrication cycles. Finally, the utilization of preceramic polymers is adaptable to complex shape configurations, and is less dependent on bulk thickness considerations.

There are three critical science issues which must be addressed to successfully synthesize useful fiber reinforced ceramics from preceramic polymers. The first issue concerns establishing conversion methodology which is adaptable to composite fabrication. The second key issue concerns the optimization of the interface characteristics between fiber and matrix to provide the necessary thermochemical stability at high temperature, and to influence the composite failure process so that strengthening and toughening are simultaneously achieved. Finally, the composite system must possess thermal and oxidative stability to prevent harmful decomposition and oxidation processes during high temperature exposures.

In this program, characterization of rheological properties, curing characteristics, and pyrolysis kinetics are utilized to define pathways for fabricating graphite fiber reinforced silicon carbide using polymethylvinylsilane precursors. Composite mechanical performance is varied primarily through the use of fiber coatings. Assessments of the converted matrix thermal stability coupled with studies of converted matrix chemistry on the microstructural level are utilized to identify polymer modifications which improve converted matrix thermal stability.

RESULTS AND DISCUSSION

Polymer precursor selections were driven by the practical desire to perform ambient pressure processing. Polymethylvinylsilanes which have been recently developed (Ref. 1) uniquely meet this need. A co-polymer supplied by Union Carbide designated Y-12044 was selected as the baseline precursor for study. The advantages of this polymer from a processing viewpoint are: low viscosity, low temperature cross-linking, and convertibility to rigid carbosilane at ambient pressure in inert atmospheres.

In the previous annual reports for this program (Refs. 2,3), extensive characterization of molecular structure, rheological behavior, and pyrolysis kinetics were documented. These studies formed the basis for developing a fabrication procedure for graphite fiber reinforced composites. The third year research effort reported herein has focused on identifying polymer modifications which lead to improved converted matrix stoichiometries.

In the following sections, the characterization data for the vinylmethylsilane supplied by Union Carbide is first summarized to provide a basis for discussion of polymer modification. This section is followed by a discussion of composite processing and the effects of processing variables on composite properties. In the final section, limitations of the Y-12044 polymer are documented, and novel polymer chemistries designed to resolve the shortcomings are characterized.

I. Y-12044 VINYLMETHYLSILANE POLYMER CHARACTERIZATION

Polymer Structure

The molecular structure of the Y-12044 polymer provided by Union Carbide was characterized using Fourier Transfer Infrared (FTIR) spectroscopy. The polymer typically produced the spectra shown in Fig. 1a. Assignments of the key features of the chemical structure are:

Frequency (cm^{-1})	Structural Group
3048	CH (vinyl)
2952, 2896	CH (aliphatic)
2078	SiH
1397, 1246	CH_3-Si
1046	SiO
1004, 937	CH_3Si
852, 770	$(CH_3)_2Si$

A schematic of the structure of the polymer is provided in Fig. 1b.

Curing Behavior

The curing characteristics of the polymer determined by differential scanning calorimetry (DSC) are provided in Fig. 2. The cross-linking exotherm, peak temperature, and heat of reaction were very similar for all lots evaluated. The FTIR spectra of cured Y-12044 is compared with the as-received polymer in Fig. 3. Polymerization of the vinyl groups is demonstrated by the virtual disappearance of the 3048 cm^{-1} peak and appearance of a third CH aliphatic peak at 2992 cm^{-1}. Problems with air sensitivity during handling are shown by the reduction of the SiH peak (2092^{-1}) and increase in the SiO peak (1050^{-1}). This indicates the extent of oxygen contamination of the resin at this stage.

Rheological Characteristics

Study of the rheological characteristics in the low temperature curing regime showed significant differences among three lots characterized. A summary of the data obtained for the polymer in the as-received and heat treated condition is provided in Table II.

The data show that the Lot 3 polymer did not respond to thermal treatment at 115°C when compared to the previous lots where significant increases in viscosity were obtained. This is significant since composite prepreg is normally B-staged by a thermal treatment to normalize hot pressing parameters.

TABLE II
VISCOELASTIC PROPERTIES OF Y-12044 POLYMER

	η_i at 40°C (poise)	η_{min} (poise)	$T_{\eta min}$ (°C)	$T_{G'=G''}$ (°C)
As-received				
Lot 1	40	2.4	104	142
Lot 2	250	6.0	108	140
Lot 3	32	2.0	103	110
After 115°C/1 hr				
Lot 1	340	24	112	127
Lot 2	1100	99	102	111
Lot 3	30	1.7	122	130

The viscoelastic behavior of the Lot 3 polymer was studied further. To simulate composite processing as closely as possible, an inert gas enclosure was arranged around the dynamic mechanical analyzer test plates. The rheological characteristics determined in inert environment for both virgin and post-thermal treatment materials are shown in Fig. 4. The viscosity minimum was extended to significantly higher temperatures when measured in the inert environment. This occurred because the oxidation reaction initiating at about 90°C, previously seen in DSC experiments, has been eliminated. Since the viscosity increased rapidly above the minimum at 153°C, heat treatments to control prepreg viscosity were investigated slightly below this temperature, around 140°C. A summary of the heat treatments tried is given in Table III. Prior fabrication experience indicated a minimum viscosity, η_{min}, between 20 to 40 poise to be a good range for B-staging the prepreg. From Table III it can be seen that treatment of 1.5 hr at 140°C was required for the Lot 3 resin.

TABLE III
EFFECT OF 140°C PRETREATMENT IN NITROGEN ON
THE VISCOSITY OF Y-12044 POLYMER

Pretreat Time	η_i at 40°C (poise)	$T_{\eta min}$ (°C)	η_{min} (poise)	Strain (%)
0	23.2	153	0.37	500
0.5	36.3	143	3.94	500
1.0	32.1	135	11.2	400
1.5	388	106	49.9	100

Pyrolysis Studies

The weight change of the polymer during heating through the curing temperature and pyrolysis regime was followed using thermal gravimetric analysis. TGA analysis for heating rates of 2°C/min and 10°C/min are shown in Fig. 5. The traces are characterized by a small volatile loss up to 200°C followed by extensive weight loss at about 350°C.

The volatile materials lost during pyrolysis were collected and analyzed. The FTIR spectrum shown in Fig. 6 shows the presence of SiH (2078 cm^{-1}) and SiO (1046 cm^{-1}) indicating significant silicon loss during pyrolysis. It is important to note the increased loss of material at the higher rate in the temperature region below 200°C. The greater low temperature loss at 10°C/min (8.6% vs 2.9%) represents evaporation of unincorporated materials. The weight loss in the 300-800°C region is due to pyrolysis of the organic polymer to a ceramic SiC phase. The lower conversion yield at higher rate (57.1% vs 62.5%) is caused by the increased loss of materials at the faster heating rate.

Experiments were performed with the Lot 3 polymer to determine the effect of cure extent on the pyrolysis rate and the solid residue yield. As shown in Fig. 2, the cure reaction initiates at about 190°C with the cross-linking exotherm peak occurring at 218°C. Cure temperatures between 200°C to 250°C were therefore selected.

Approximately 50 gm of the methylvinylsilane were cured in inert atmosphere according to the schedules described in Table IV. All cured samples were solid with little evidence of porosity due to foaming. Density was approximately 1.01 gm/cm^3.

TABLE IV
CURE CYCLES FOR VINYLMETHYLSILANE POLYMER

Sample	Cure Cycle	
200/1	1	RT → 200°C (5°C/min) hold 1 hr
250/1	2	RT → 250°C (5°C/min) hold 1 hr
250/6	3	Cycle 2 plus RT → 250°C (20°C/min) hold 5 hr
250/12	4	Cycle 3 plus RT → 250°C (20°C/min) hold 5 hr

The weight loss during cure, measured on an analytical balance, is shown in Table V. Note that small weight losses on the order of 1% are observed in comparison with approximately 5% weight loss of samples evaluated in the TGA. This discrepancy is probably due to the extreme difference in surface to volume ratios of the two samples. The TGA samples are on the order of 15 mg and are exposed in open platinum boats while the 50 gm cure samples were heated in partially closed vessels. Thus, low molecular weight species which would otherwise be lost by volatilization could be retained and incorporated into the cross-linked matrix.

TABLE V
WEIGHT LOSS DURING CURE

Sample	% Wt. Loss
200/1	0.99
250/1	0.50
250/6	0.75
250/12	1.05

Each of the four cured specimens were ground into powder and evaluated in the TGA with heating rates of 2, 5, and 10°C/min to 1000°C under nitrogen atmosphere. The pyrolysis residues at 1000°C as a function of heating rate and cure schedule are summarized in Table VI. The data show that the cure schedule utilized had little effect on the final residue yield. Lower heating rates, however, improved the residual yield. It was concluded that curing for 1 hr at 200°C was a sufficient treatment for optimum pyrolysis yield, and the yield was primarily dependent upon the pyrolysis rate.

TABLE VI
RESIDUE AFTER HEATING TO 1000°C

	Residual Weight		
Sample	2°C/min	5°C/min	10°C/min
200/1	67.9	67.4	65.2
250/1	70.7	65.0	63.4
250/6	66.7	64.7	66.6
250/12	68.0	66.0	64.0

Compositional analysis of the ceramic phase produced by pyrolysis of Y-12044 at 800°C was performed using Auger electron spectroscopy. The results are given in Fig. 7. The elemental ratio of Si:C is shown to be about 1:2 and considerable oxygen contamination is indicated (6-10%).

X-ray diffraction analysis of the 800°C pyrolyzed product indicated a near amorphous, microcrystalline structure as evidenced by very diffuse peaks about the primary β-SiC peaks. After heating to 1500°C, the β-SiC peaks were clearly evident, but were significantly broadened.

Conversions of bulk samples of Y-12044 were carried out to determine the dimensional stability of parts during the conversion process, and the density of the resultant ceramics. Pieces of cured Y-12044 were directly converted at 850°C. In addition, parts were molded using ceramic powders preprocessed from cured Y-12044 which was powdered and then pyrolyzed at 550°C and 850°C. Bulk pieces were prepared from powders bound together with the Y-12044 resin. These preceramic compacts were pyrolyzed at 850°C. Observations and measured densities are summarized in Table VII. The results show severe distortion of parts molded from cured Y-12044 resin. Pyrolysis of the powder compacts relieved most of the distortion and optimized density. Some contraction was seen with parts made from the preconverted 550°C powder, while the pieces made from fully converted, 850°C SiC powder showed dimensional stability. Densities of all parts were substantially lower than expected for amorphous SiC (~2.6 g/cm^3) or β crystalline SiC (~3.2 g/cm^3).

TABLE VII
DENSITY AND DIMENSIONAL STABILITY OF
METHYLVINYLSILANE PYROLYZED AT 800°C

Sample	Density (g/cm^3)	Dimensional Change
Cured Y-12044 Lot 3	1.83	Severe distortion, about 30% shrinkage of dimensions
87% 550°C phase + Y-12044 Lot 3	2.03	Symmetrical 20% shrinkage of dimensions
90% 850°C phase + Y-12044 Lot 3	2.04	<1% dimensional change

II. COMPOSITE SYNTHESIS

Based on the Y-12044 polymer characterization data, a fabrication procedure was defined for producing carbon fiber reinforced SiC composites. The procedure utilized the following steps. Heat stabilized 8-harness satin weave T-300 fabric was first impregnated with Y-12044 polymer in inert atmosphere. The resin impregnated fabric was stacked in a mold and densified under 100 psi pressure in a vacuum bag while heating to 220°C over an 8 hr period. The composites were cured for 2 hrs at 220°C. The cured composites were then pyrolyzed by heating in inert atmosphere to 800°C over a 20 hr period. The pyrolyzed parts were then pressure impregnated with polymer at 100 psi, pressure cured in an autoclave at 220°C under 100 psi Argon, and heated to 800°C over 20 hrs. Following each reimpregnation and pyrolysis cycle, the panels were post heat treated by heating to 1400°C over an 8 hr period and holding for 1 hr at 1400°C.

This generic fabrication procedure was modified in several ways. To enhance fiber-matrix bonding, CVD SiC coatings were utilized on the fabric. To enhance densification, orthoboric acid wash was utilized between polymer impregnation cycles. Finally, alternating polymer reimpregnation using one cycle of polysilazane (Huls T3812) followed by two cycles of the Y-12044 was utilized to vary densification.

The composites fabricated and evaluated in the third year, utilized the orthoboric acid wetting agent and alternating polymer reimpregnation (one cycle polysilazane followed by two cycles of Y-12044) as a densification procedure. The properties obtained with uncoated T-300 fabric and silicon carbide coated T-300 fabric are compared in the following sections.

Physical Properties

The physical properties of these two panels are listed in Table VIII. There was minimal variation in density measured on individual specimens cut from the panels. It is believed that the use of a wetting agent during each reimpregnation cycle provides significant advantage in this respect. The panel incorporating coated fabric had a significantly higher density due to reduced ply thickness.

TABLE VIII
COMPOSITE PHYSICAL PROPERTIES

Panel	Fiber Volume %	Average Density (gm/cm^3)
10195-41	0.465	1.68
10195-63	0.533	1.72

Typical microstructures from these two panels are presented in Figs. 8 and 9. The higher density 10195-63 panel incorporating the coated fabric was better bonded. Void area between plies was reduced, and as shown in the higher magnification micrographs, fiber/matrix bonding within bundles was improved. It was also noted in the 10195-63 panel that the individual fibers appeared more irregular as if they were attacked in some way during the coating step.

Ultrasonic velocity profiles measured for these two panels are summarized in Table IX. The longitudinal and transverse velocities were comparable. The through-thickness velocity for the panel incorporating coated fabric was significantly higher suggesting improved bonding.

TABLE IX
ULTRASONIC VELOCITY STATISTICS

	10195-41	10195-63
Longitudinal		
Average (in/μsec)	.2846	.2837
Data pts	2	2
Transverse		
Average (in/μsec)	.2861	.2804
Data pts	3	2
Across-Ply		
Average (in/μsec)	.1010	.1291
Data pts	6	3

Mechanical Properties

The tensile stress-strain characteristics determined at 20°C are summarized in Table X and are compared in Fig. 10. The specimen from panel 10195-63

incorporating coated fabric was extremely brittle failing at a tensile strain of 0.0005. The different tensile failure modes of these composites are demonstrated macroscopically in Fig. 11. In the case of the tensile specimens from panel 10195-41, the fracture is more fibrous indicative of a weak fiber/matrix interface. In contrast, the tensile specimen from panel 10195-63 exhibited catastrophic failure through the composite cross-section once a crack was initiated. This is typical of strongly bonded composites.

TABLE X
TENSILE PROPERTIES AT 20°C

Panel	Specimen Density	Ultimate Tensile Strength (psi)	Elastic Modulus (Msi)	Strain to Failure (%)
10195-41	1.680	37680	10.27	0.59
	1.687	36610	11.58	0.47
10195-63	1.721	5250	11.48	0.05

The compressive stress-strain characteristics are summarized in Table XI and are compared in Fig. 12. The compression strength of specimens from panel 10195-63 incorporating coated fabric were significantly higher due to a much higher strain to failure. These results are consistent with a higher fiber/matrix bond strength achieved with the coated fabric.

TABLE XI
COMPRESSIVE PROPERTIES AT 20°C

Panel	Specimen Density	Ultimate Compression Strength (psi)	Compression Modulus (Msi)	Strain to Failure (%)
10195-41	1.680	19400	10.16	0.28
	1.681	19900	10.20	0.31
	1.682	20320	11.09	0.27
10195-63	1.721	38400	10.49	0.39
	1.709	35200	10.0	0.40
	1.705	38400	10.42	0.36

The compressive failure modes are compared in Fig. 13. The side views show that both specimens failed in shear. However, in specimens from panel 10195-41 with weak fiber/matrix bonding, the failure zone also exhibited significant intralaminar failure. In the composite with the strong fiber/matrix interface, panel 10195-63, the failure zone was more confined to the shear plane.

The interlaminar shear strengths are summarized in Table XII. The shear strength exhibited by the panel incorporating coated fabric was an order of magnitude higher than the other panel again reflecting the higher fiber/matrix bond strength.

TABLE XII
INTERLAMINAR SHEAR STRENGTH AT 20°C

Panel	Specimen Density (gm/cm^3)	Interlaminar Shear Strength (psi)
10195-41	1.664	350
	1.689	300
10195-63	1.725	2820
	1.725	4060
	1.720	2980

Comparison with Previous Results

The composite properties achieved as a function of various processing parameters over the course of this three year program are compared in Table XIII. Several trends may be discerned. The use of wetting agents maximized density. Proper fabric heat stabilization maximized tensile strength. Fiber coatings dramatically improved interlaminar shear and compression properties, but degraded tensile properties. The peak pyrolysis temperature (800°C vs. 1400°C) did not seem to affect the mechanical properties. The use of alternating the polysilazane and methylvinylsilane resins improved the final density. It may be seen in the fifth generation panel where all positive benefits were combined, that the fiber-matrix interface strength was too high resulting in a brittle failure mode in tension. However, the shear and compression properties were dramatically improved.

It was concluded from these fabrication experiments that composites with a good combination of tensile, shear, and compression strength could be fabricated using the polymer pyrolysis approach with appropriate control of fiber-matrix bonding and densification procedures.

TABLE XIII
CARBON FIBER REINFORCED SIC DERIVED
FROM POLYMER PRECURSORS

	First Generation	Second Generation	Third Generation	Fourth Generation	Fifth Generation
Fiber vol %	51	43	47	46	53
Density (gm/cm^3)	1.71	1.61	1.60	1.68	1.72
Tensile strength(ksi)	23.5	43.6	31.5	37.1	5.25
Elastic modulus(Msi)	11.2	10.9	8.7	10.9	11.5
Comp. strength(ksi)	8.7	8.7	18.1	19.9	34.0
ILS (psi)	540	450	1160	325	3290
ILT (psi)	110	<100	-	-	-
Processing variable	(1)(4)(7)	(2)(4)(7)	(2)(3)(4)(7)	(1)(2)(5)(6)	(1)(2)(3)(5)(6)

(1) Wetting agents to improve densification
(2) Proper fabric heat stabilization
(3) Fabric coating
(4) Y-12044 polymer reimpregnation
(5) Alternating reimpregnation: Y-12044/silazane
(6) Pyrolyzed to 800°C
(7) Pyrolyzed to 1400°C

III. DEVELOPMENT AND EVALUATION OF IMPROVED POLYMER PRECURSORS

The results reported in Section I showed that the Y-12044 methylvinylsilane polymer supplied by Union Carbide was extremely sensitive to oxygen absorption, and produced a pyrolyzed product which was carbon rich and oxygen contaminated even under controlled processing conditions. The presence of Si-H groups was correlated with oxygen contamination. The volatilization of silicon fragments with a corresponding lowering of yield and stoichiometry during pyrolysis was believed to be caused by the presence of non-reactive Me_3Si end groups. As a basis for further development, a SiH free methylvinylsilane provided by Union Carbide and similar methylvinylsilane polymers with reactive end group substitutions developed at UTRC were evaluated.

A. SIH FREE Y-12044 POLYMER

A test polymer containing only incidental SiH was prepared by Union Carbide for evaluation. This polymer was designated Y-12044NH. The evaluation of this polymer was reported in detail in Ref. 3. Important findings are summarized here to aid subsequent discussions.

The structure of Y-12044NH polymer and its FTIR spectrum are shown in Fig. 14. This polymer produced a spectrum similar to the Y-12044 Lot 3 polymer FTIR spectrum shown in Fig. 1 with the exception that most of the SiH (2078 cm-1) absorption peak is absent.

Pyrolysis of Y-12044NH gave substantially reduced yields of the high temperature ceramic phase, typically 37-40%. Further experiments demonstrated pyrolysis of carefully precured samples could raise the conversion to 49-51%. These conversions compared with the 62-64% ceramic conversions obtained from the SiH containing Y-12044 resins.

Bulk and rheometric curing studies indicated the curing of Y-12044NH occurred at temperatures substantially higher than the Y-12044 polymer. Complete curing of SiH containing Y-12044 could be achieved quickly at 195°C while Y-12044NH remained uncured for extended reaction times at 230°C. Eventual curing above 230°C resulted in porous samples indicative that some decomposition of the resin had occurred.

A series of initiators and accelerators were evaluated to lower the curing temperature of Y-12044NH. This approach attempted to lower the initiation temperature of the vinyl crosslinking reaction (initiator) and to accelerate the crosslinking by use of mobile reactive components (accelerators). The most successful systems are described in Table XIV. The rheology of the accelerated Y-12044NH is compared with as-received Y-12044NH in Fig. 15. Pyrolysis yields of the Y-12044NH polymers were reduced relative to Y-12044 due to release of organosilanes during the pyrolysis reaction.

TABLE XIV
MODIFIED Y-12044NH CURING TEMPERATURES

System	Cure Temp. (°C)
Y-12044 Lot 3	185
Y-12044NH	220
Y-12044NH (1% TBP)	165
Y-12044NH (5% BTMSA)	195
Y-12044NH (5% BDMVSE)	185
Y-12044NH (0.5% TBP + 5% BTMSA)	155

TBP = t-Butyl Peroxide
BTMSA = Bis(Trimethylsilyl)-acetylene
BDMVSE = Bis(Dimethylvinylsilyl)-ethane

Analysis of accelerated Y-12044NH converted to a ceramic SiC phase at 800°C was performed using Auger analysis. The results are shown in Fig. 16. Although this material showed reduced oxygen contamination (3-5%), the Si:C ratio was typically 1:2 indicating substantial free carbon content as with the Y-12044.

B. REACTIVE ENDGROUP POLYMETHYLVINYLSILANE POLYMERS

A family of experimental polymethylvinylsilane polymers have been under development at UTRC with the intent of providing air stable polymers which convert to solids of improved stoichiometry. The molecular design has eliminated SiH groups to control oxygen absorption and incorporated vinyl endgroups to control loss of key volatiles during pyrolysis. Synthesis chemistry was developed to incorporate reactive dimethylvinylsilyl endgroups on a methylvinylsilane polymer backbone. One of these polymers, designated W1-164, was selected for evaluation in this program.

Polymer Structure (W1-164)

The molecular structure of the endblocked polymer is shown in Fig. 17a and its FTIR spectrum is given in Fig. 17b. This polymer shows increased free vinyl content, minimal SiH presence (2080 cm^{-1}), and low values of oxygen contamination associated with the SiO peak (1050 cm^{-1}).

Curing Behavior and Rheology

The curing characteristics analyzed by DSC are shown in Fig. 18. The vinyl crosslinking exotherm shows a broad peak in the 230-310°C range which is considerably smaller than the crosslinking exotherm observed for Y-12044. However, the exotherm appears to extend to a lower limit of 150°C suggesting existence of vinyl groups in varying environments. Bulk curing of the W1-164 polymer at 195-210°C yields a partially cured pliable material supporting this viewpoint. The viscoelastic behavior of this resin is shown in Fig. 19. The resin cures in the 175-180°C range. Use of t-Butyl peroxide catalyst allows curing at lower temperatures to more rigid solids at around 150°C.

Pyrolysis Studies

The weight change of the polymer during heating through the curing and pyrolysis regimes was followed by thermal gravimetric analysis. Data generated at heating rates of 2°C/min and 10°C/min in nitrogen are shown in Fig. 20. The traces are characterized by a weight loss of volatile uncured material at lower temperatures up to 200°C. Majority of the conversion of the cured resin occurs at 400-600°C as shown by the pyrolysis weight loss in this range with minor weight loss occurring to about 800°C. The greater yield of ceramic at 2°C/min (54% vs 48%) was due to increased loss of material at the faster heating rate.

Compositional analysis of the ceramic phase converted at 850°C was performed by Auger electron spectroscopy. The results are given in Fig. 21. The elemental Si:C ratio is about 1:2.8 which is more carbon rich than the Y-12044 derived ceramics. The oxygen level was about 5.5%.

C. BULK CERAMIC THERMAL STABILITY

In an effort to evaluate the high temperature stability of the pyrolyzed polymers, bulk pieces which had been pyrolyzed at 850°C were subjected to further heating to 1440°C in a thermal balance. The Y-12044 baseline precursor was compared with the W1-164 precursor. Bulk samples were prepared using the following procedure. The polymers were pyrolyzed at 810°C, and the converted phases were powdered. The pyrolyzed powders were then bound with virgin polymer, and cured under pressure in a mold. The cured samples were then pyrolyzed by heating at 2°C/min to 900°C and holding for 1 hr.

The bulk ceramics were then evaluated in the mass balance by heating at 2°C/min to a temperature of 1440°C and holding for 8 hrs at 1440°C in nitrogen atmosphere. The data obtained during the heating cycle to 1440°C at a rate of 2°C/min is shown in Fig. 22. The Y -12044 derived ceramic exhibited significant mass changes which initiated at approximately 1200°C. At 1440°C, an 11.8% mass loss was recorded. The W1-164 ceramic was significantly more stable. An overall mass loss of only 1.21% was recorded. The mass changes for the converted products during the 8 hr isothermal hold at 1440°C are shown in Fig. 23. The Y-12044 derived ceramic continued to lose weight, exhibiting an overall mass loss of 48.0% after the 8 hr hold. In contrast, the W1-164 derived ceramic was remarkably stable, exhibiting a mass loss of only 2.48% after the isothermal hold at 1440°C. Continued heating to 1500°C resulted in only small additional mass losses.

XRD analysis indicated that both polymer conversions were amorphous after initial pyrolysis to the temperature range of 850-900°C. After heating to 1500°C, the presence of broad β-SiC peaks was evident indicating the converted ceramic to be a mix of microcrystalline and amorphous phases. The XRD patterns for the W1-164 converted products are presented in Fig. 24.

D. CONVERTED PRODUCT PHASE DISTRIBUTION

The converted ceramics from the Y-12044 and W1-164 precursors were studied using X-ray Photoelectron Spectroscopy (XPS) to obtain an approximate description of the phases present. Atomic fractions were calculated from the XPS survey spectra obtained from fresh fracture surfaces using elemental peak area measurements normalized by appropriate sensitivity factors. A summary of the atomic concentrations determined by this technique is presented in Table XV. It is noted that the oxygen level was considerably reduced in W1-164 product pyrolyzed at 850°C compared to the Y-12044 product pyrolyzed at 900°C.

TABLE XV
ATOMIC CONCENTRATIONS DETERMINED
FROM XPS SURVEY SPECTRA

Source Polymer	Conversion Temperature (°C)	C	O	Si	Other
Y-12044	900	42.2	32.1	25.3	0.4
Y-12044	1500	30.7	28.7	40.5	0.1
W1-164	850	64.0	10.7	24.9	0.4

To determine how the elemental species were bound, curve fitting analyses of the carbon 1s and silicon 2p peaks was performed. The approach taken was to fix the SiO_2, C, and SiC peak positions at binding energies typically reported in the literature, i.e,. for Si-2p peaks, SiO_2 at 103.4-103.6 eV and SiC at 100.4 eV, and for C-1s peaks, C at 284.6-285.0 eV and SiC at 282.6 eV. In addition, the full width at half maximum was defined as 1.8 eV. Following assignment of these values, curve fitting was then performed to derive the components of the experimental peaks obtained.

Presented in Fig. 25 are the analyses of the carbon 1s and silicon 2p peaks determined for the Y-12044 ceramic converted at 900°C. Silicon was bound as SiC, SiO_2, and a Si-O-C complex. The shape of the carbon peak also indicated considerable retention of free carbon within the structure. On the basis of the curve fit analysis and the overall chemistry, the distribution of various elements in the microstructure was derived. This is presented in Table XVI. High levels of oxygen are bound to free carbon in the structure, and a Si-O-C complex appears to be the dominant phase.

TABLE XVI
DISTRIBUTION OF ELEMENTS WITHIN THE
Y-12044 PRODUCT CONVERTED AT 900°C

Element	Atomic Percent	Distribution (a/o)
O	32.1	
C	42.2	11.3 as C 4.5 as C-O 2.3 as C=O, O-C-O 19.1 as Si-O-C 5.1 as SiC
Si	25.3	1.6 as SiO2 17.1 as Si-O-C 6.5 as SiC

The analyses of the Y-12044 ceramic converted at 1500°C are shown in Fig. 26. Inspection of the carbon 1s peak indicates that carbon bound oxygen complexes are eliminated as well as a significant amount of the free carbon. This is consistent with the large mass loss above 1200°C shown in Fig. 22, and is attributed to volatilization of CO and CO_2 from the microstructure. The curve fit analyses summarized in Table XVII indicated the majority of the microstructure was composed of a Si-O-C complex with a small amount of SiC.

This analysis, however, is inconsistent with the XRD analysis which showed development of broad β-SiC peaks after the 1500°C pyrolysis. If a chemical shift of the C-1s and Si-2p peaks to values of 283.3 eV and 101.3 eV was assumed for SiC, then the alternate curve fit analysis shown in Table XVIII was obtained. Note the dominant phase was now SiC with a significant amount of SiO_2 and relatively low level of free carbon.

TABLE XVII
DISTRIBUTION OF ELEMENTS WITHIN THE
Y-12044 PRODUCT CONVERTED AT 1500°C

Element	Atomic Concentration	Distribution (a/o)
O	28.7	
C	30.7	3.1 as C 26.3 as Si-O-C 1.3 as SiC
Si	40.6	8.7 as SiO2 30.5 as Si-O-C 1.3 as SiC

TABLE XVIII
ALTERNATE CURVE-FIT ANALYSIS OF Y-12044 PYROLYZED
AT 1500°C ASSUMING 0.7 eV CHEMICAL SHIFT

Element	Atomic Concentration	Distribution (a/o)
O	28.7	
C	30.7	3.0 as C[1] 27.7 as SiC[1]
Si	40.6	9.6 as SiO2[1] 30.9 as SiC[1]

[1] alternate analysis assuming 0.7 eV chemical shift

Finally, the converted product from the W1-164 polymer was evaluated. The results of the curve-fit analyses are shown in Fig. 27 and listed in Table XIX. This analysis shows a higher level of free carbon in the pyrolyzed product compared to the Y-12044 ceramic as well as a significant amount of the Si-O-C complex. The overall level of oxygen containing species is significantly lower than in Y-12044.

TABLE XIX
DISTRIBUTION OF ELEMENTS WITHIN THE
W1-164 PRODUCT CONVERTED AT 850°C

Element	Atomic Concentration	Distribution (a/o)
O	10.7	
C	64.0	39.0 as C 7.1 as C-O 17.0 as Si-O-C 0.9 as SiC
Si	24.9	4.2 as SiO2 19.5 as Si-O-C 1.2 as SiC

It is evident from this preliminary analysis that XPS can be a valuable tool for following changes in atomic concentration and their compound distribution within these pyrolyzed microstructures. However, it is also clear that interpretation of the results using curve fitting techniques is not precise due to possible chemical shift effects. Significant effort is required with standards of better known chemistry to allow the full potential of the technique to be realized.

SUMMARY AND CONCLUSIONS

A characterization methodology encompassing measurements of curing characteristics, rheological properties, and pyrolysis kinetics was utilized to establish a composite fabrication cycle for a commercially supplied methylvinylsilane polymer designated Y-12044. Using this precursor, carbon fabric reinforced "silicon carbide" matrix composites were fabricated and evaluated. The term "silicon carbide" is used rather loosely here since the pyrolyzed matrix microstructures consisted of SiC, SiO_2, and Si-O-C complexes. Composites exhibiting a range of mechanical performance were demonstrated through the use of wetting agents, fiber coatings, and reimpregnation variations.

The primary shortcomings of the commercially available polymer were identified as severe oxygen contamination during processing and excess carbon in the pyrolyzed product. XRD, Auger, and XPS analyses showed that the 900°C pyrolyzed product was an amorphous ceramic consisting primarily of a Si-O-C complex with some free carbon, and small amounts of SiO_2 and SiC. On heating the converted ceramic further, instabilities associated with CO and CO_2 release initiated at about 1200°C. The ceramic pyrolyzed at 1440°C showed an increase in β-SiC and SiO_2 content at the expense of the Si-O-C.

Polymer chemistry modifications were investigated to improve the oxygen sensitivity of the polymer and the stoichiometry of the pyrolyzed product. Removal of endgroups from the methylvinylsilane baseline polymer reduced oxygen contamination, but carbon to silicon ratio remained at 2:1 and did not improve thermal stability. Novel methylvinylsilanes with reactive endgroups were shown to be air-stable curable polymers with ceramic convertibility >60%. The pyrolysis products from the reactive endgroup methylvinylsilanes exhibited reduced oxygen content, but an increase in overall carbon content in the microstructure. Analysis again showed SiC, SiO_2, and Si-O-C complexes as primary microstructural components. The converted products from these novel polymers exhibited remarkable thermal stability at temperatures up to 1500°C.

The program demonstrated that while useful composites can be fabricated with existing polymeric precursors, significant improvements in converted product stoichiometry and thermal stability can be anticipated through molecular adjustments. Recommendations for future research focus on two

activities. First, it is important to evaluate the environmental stability of matrices and composites derived from polymeric precursors. It is clear from the XPS studies that these materials exhibit very complex bonding schemes and are not simply phase pure mixtures of known compounds. Second, a strong program to investigate innovative precursor chemistries and novel processing approaches is recommended to pursue the goal of achieving controlled stoichiometry and microstructure in pyrolyzed polymers which can serve as matrices for high temperature ceramic composites.

REFERENCES

1. "Organosilane Polymers IV, Polycarbosilane Precursors for Silicon Carbide," C. L. Schilling, J. P. Wesson, and T. C. Williams, J. Polym. Sci., Polym. Symp. 70, 121 (1983).

2. "A Study of the Critical Factors Controlling the Synthesis of Ceramic Matrix Composites from Preceramic Polymers," J. R. Strife, J. P. Wesson, R. A. Pike, and H. H. Streckert, AFOSR Contract F49620-87-C-0093, Annual Technical Report (1988).

3. "A Study of the Critical Factors Controlling the Synthesis of Ceramic Matrix Composites from Preceramic Polymers," J. R. Strife, J. P. Wesson, R. A. Pike, and H. H. Streckert, AFOSR Contract F49620-87-C-0093, Annual Technical Report (1989).

R90-917810-5

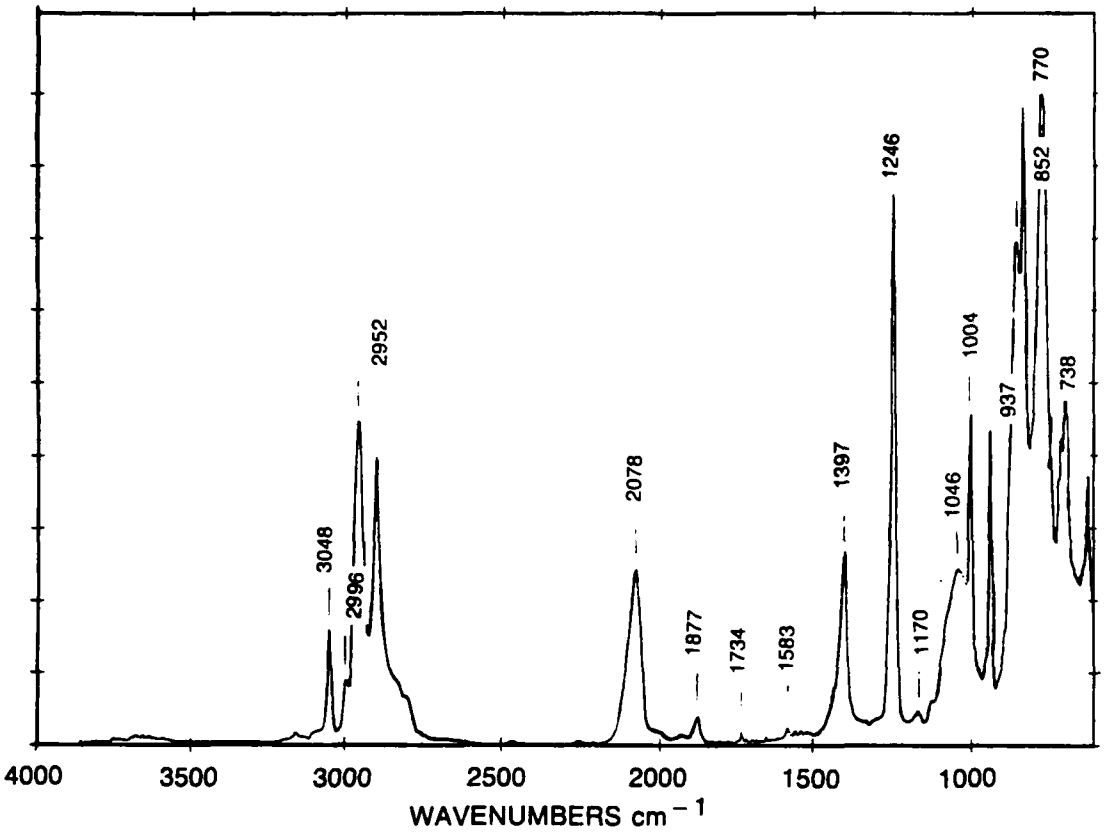

Figure 1a. FTIR spectrum for as-received Y-12044 polymer - Lot 3.

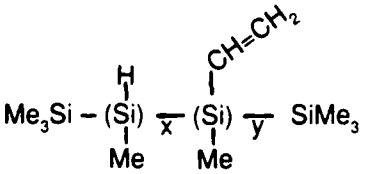

Figure 1b. Structure of the Y12044 co-polymer.

90-6-33-6

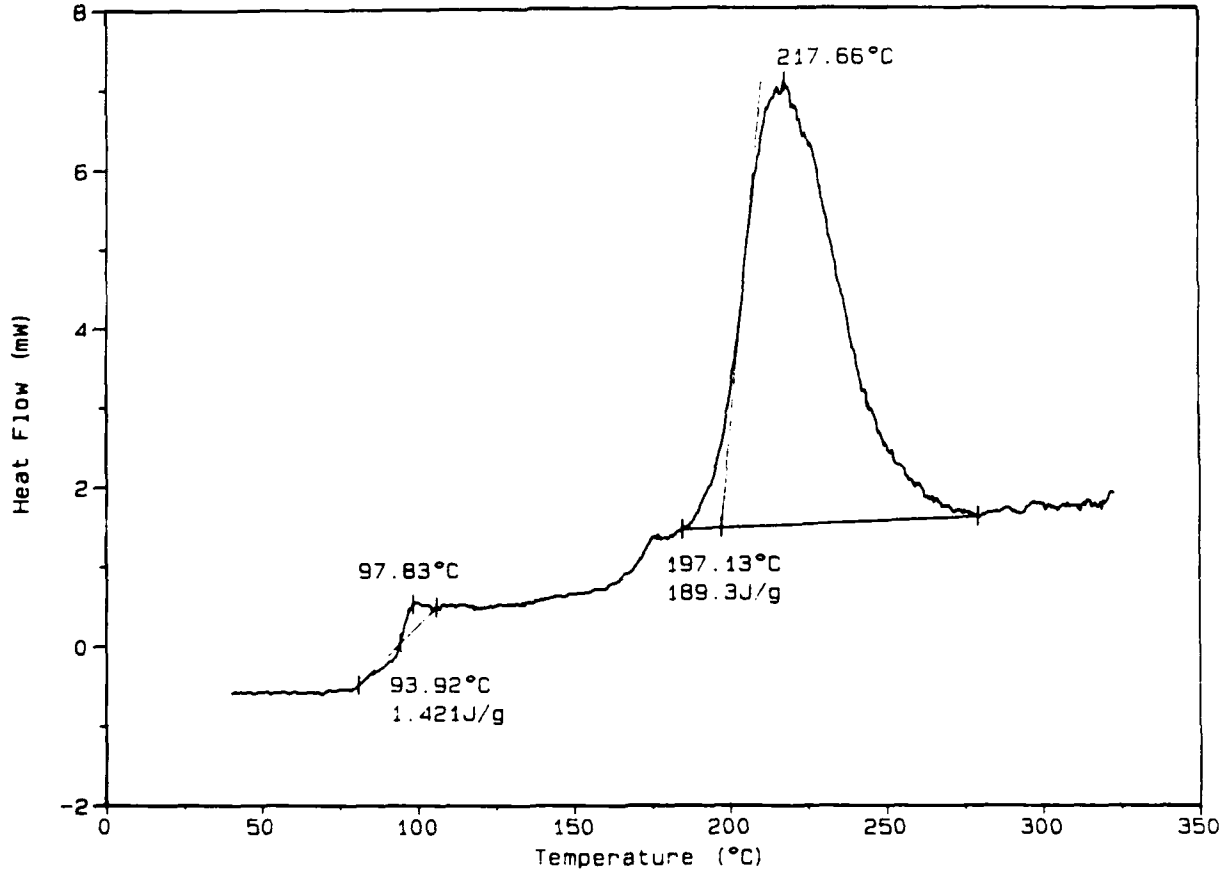

Figure 2. Heat flow as a function of temperature in nitrogen atmosphere for Lot 3 Y-12044 polymer.

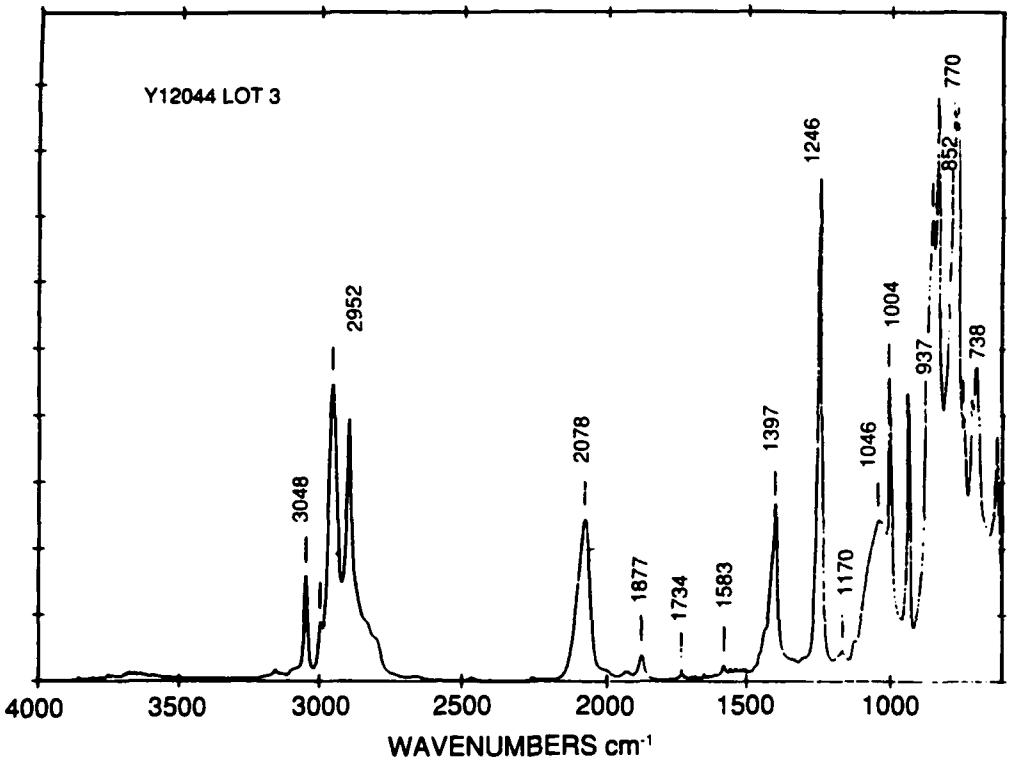

(a) AS-RECEIVED POLYMER

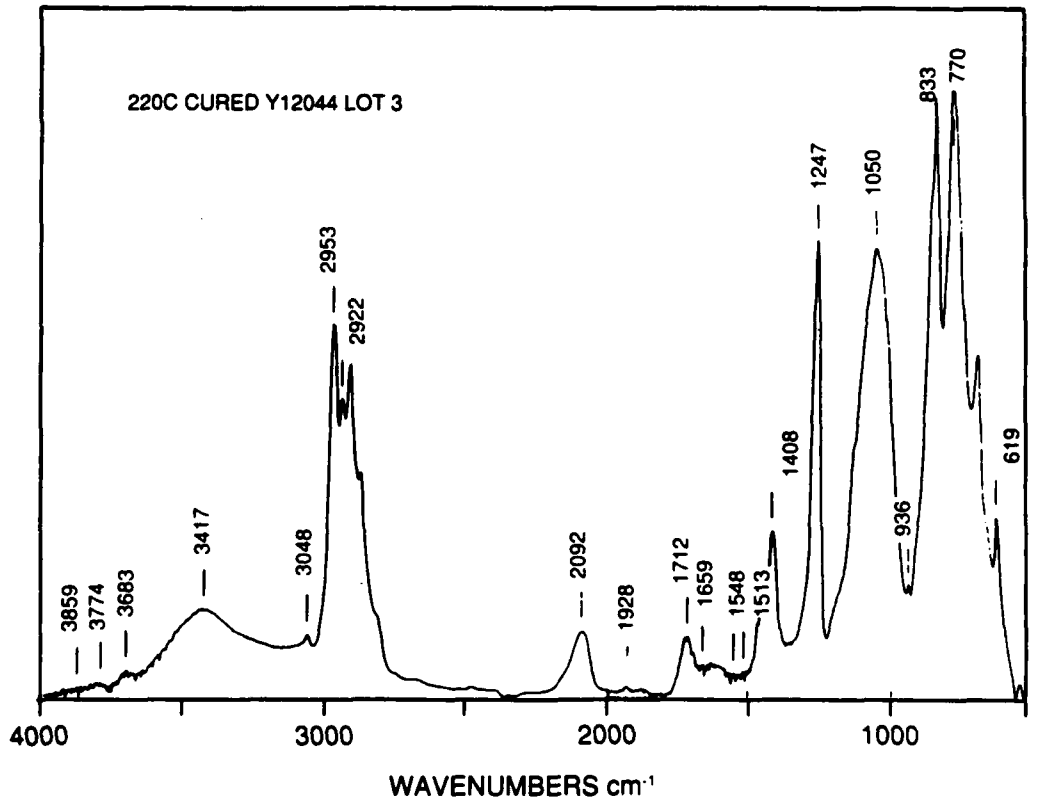

(b) CURED AT 220°C IN ARGON

Figure 3. FTIR spectra of lot 3 Y-12044

90-2-44-4

R90-917810-5

a) AS-RECEIVED

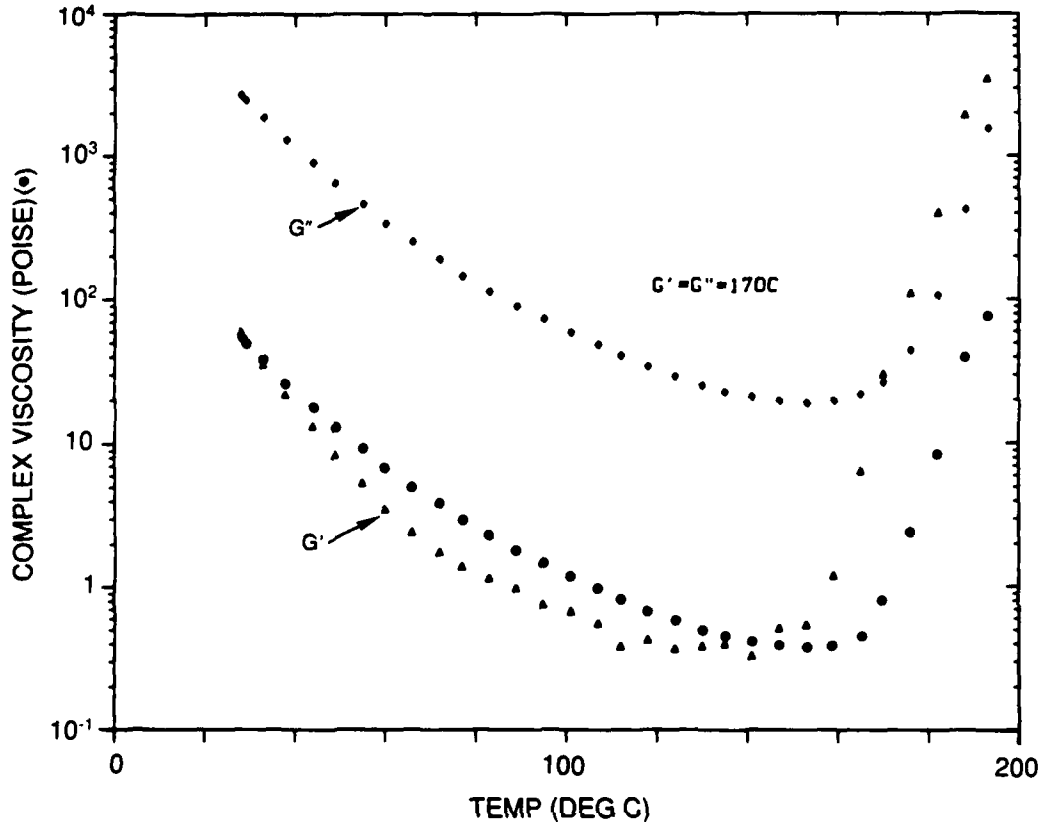

b) 1 hr AT 140°C

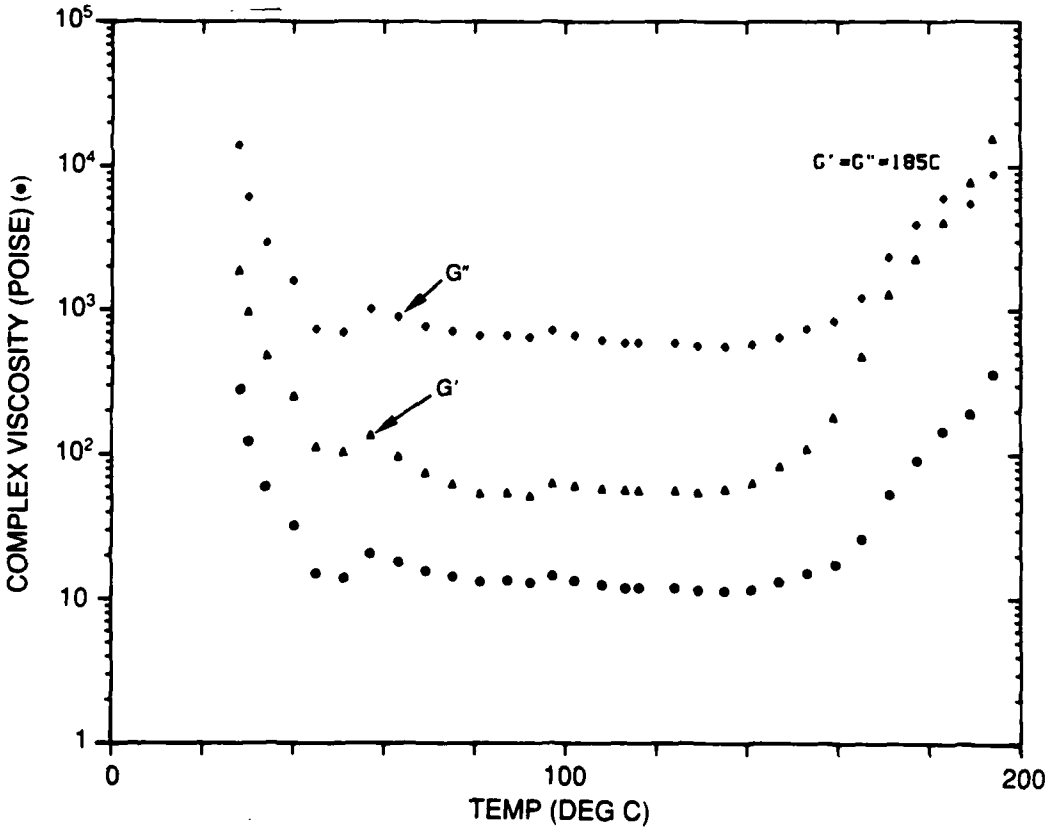

Figure 4. Viscoelastic response of Lot 3 Y-12044 polymer in inert cell.

89—8—29—6

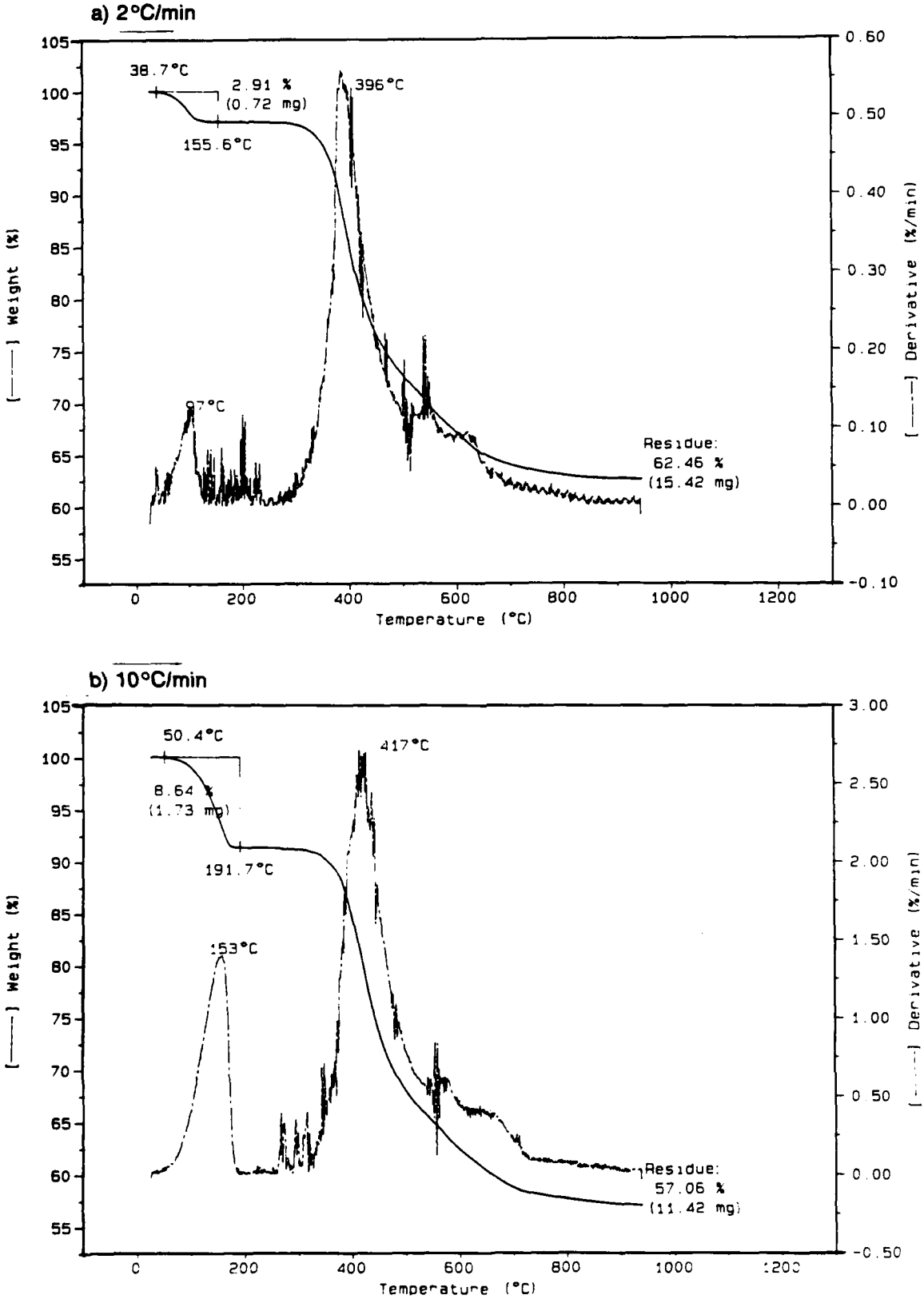

Figure 5. Thermogravimetric data for Lot 3 Y-12044 polymer as a function of heating in nitrogen atmosphere.

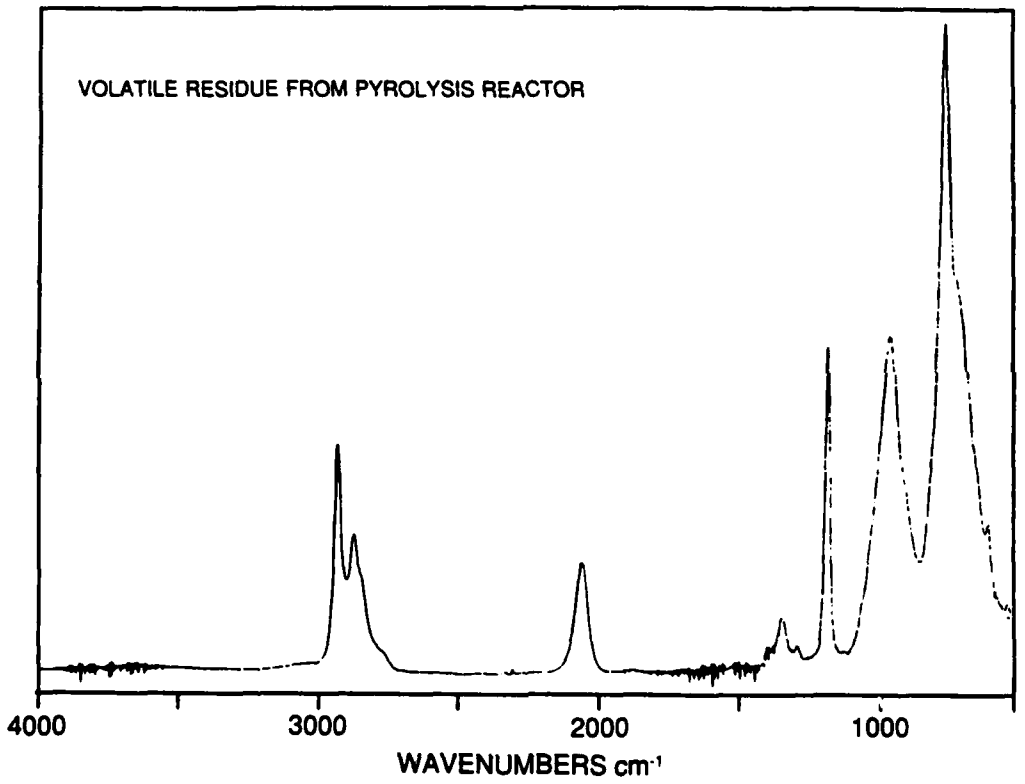

Figure 6. FTIR spectrum of volatile residue from pyrolysis reactor.

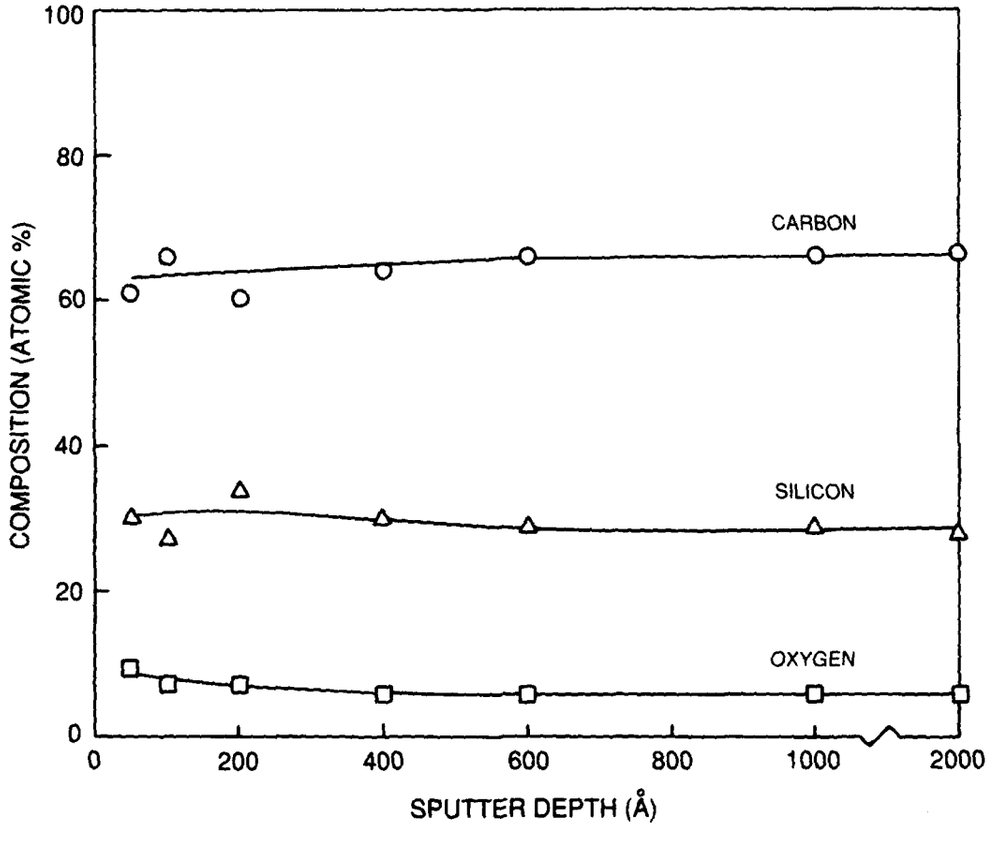

Figure 7. Auger analysis of fracture surface of Y-12044 derived 800°C pyrolysis product.

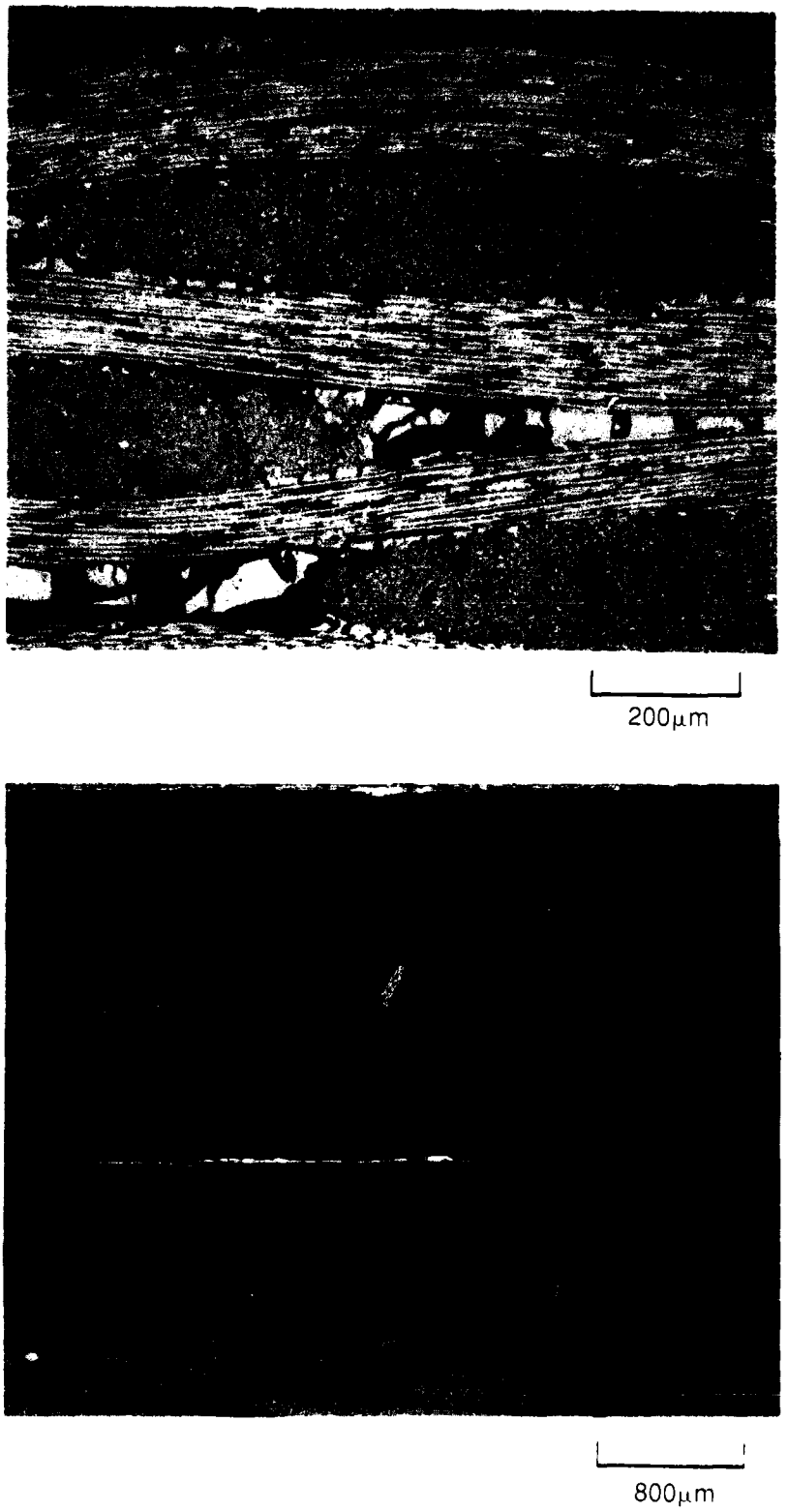

Figure 8. T-300 carbon fiber reinforced CMC derived from polysilazane/methylvinylsilane impregnation and pyrolysis. (Panel 10195-41).

200μm

800μm

Figure 9. Silicon carbide coated T-300 fiber reinforced CMC derived from polysilazane/methylvinylsilane impregnation and pyrolysis. (Panel 10195-63).

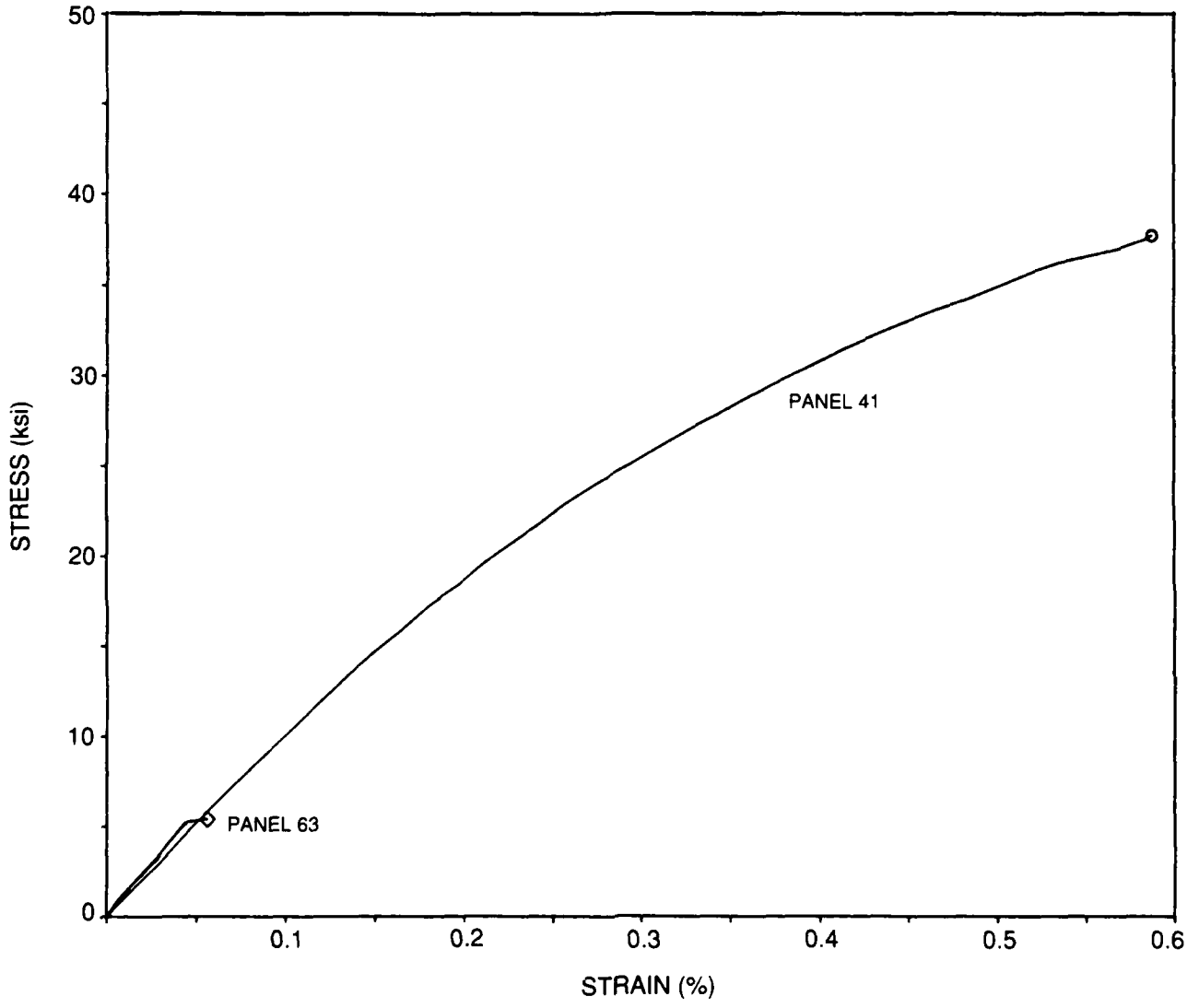

Figure 10. Tensile response at 20°C for 2D carbon fiber reinforced CMC derived from polysilazane/methylvinylsilane.

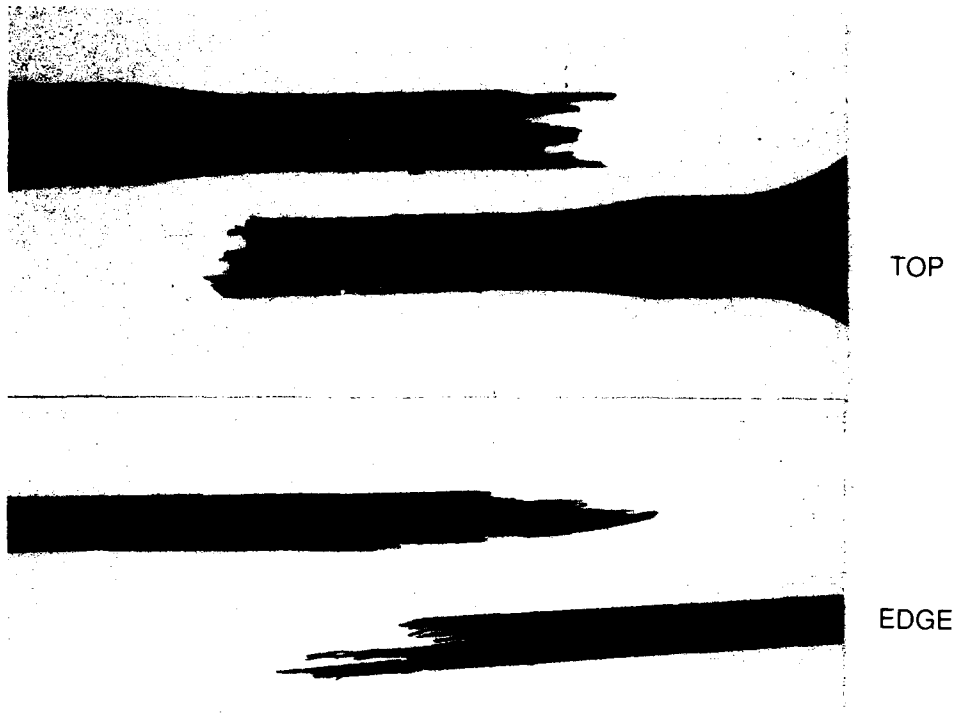

(a) PANEL 10195-41

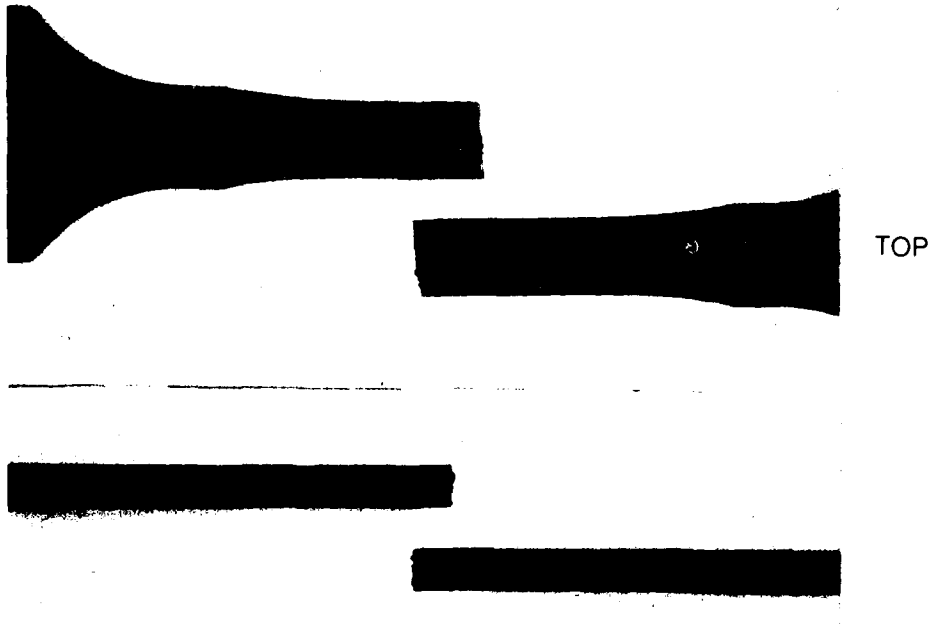

(b) PANEL 10195-65

Figure 11. Comparison of tensile fracture modes.

91-1-4-4

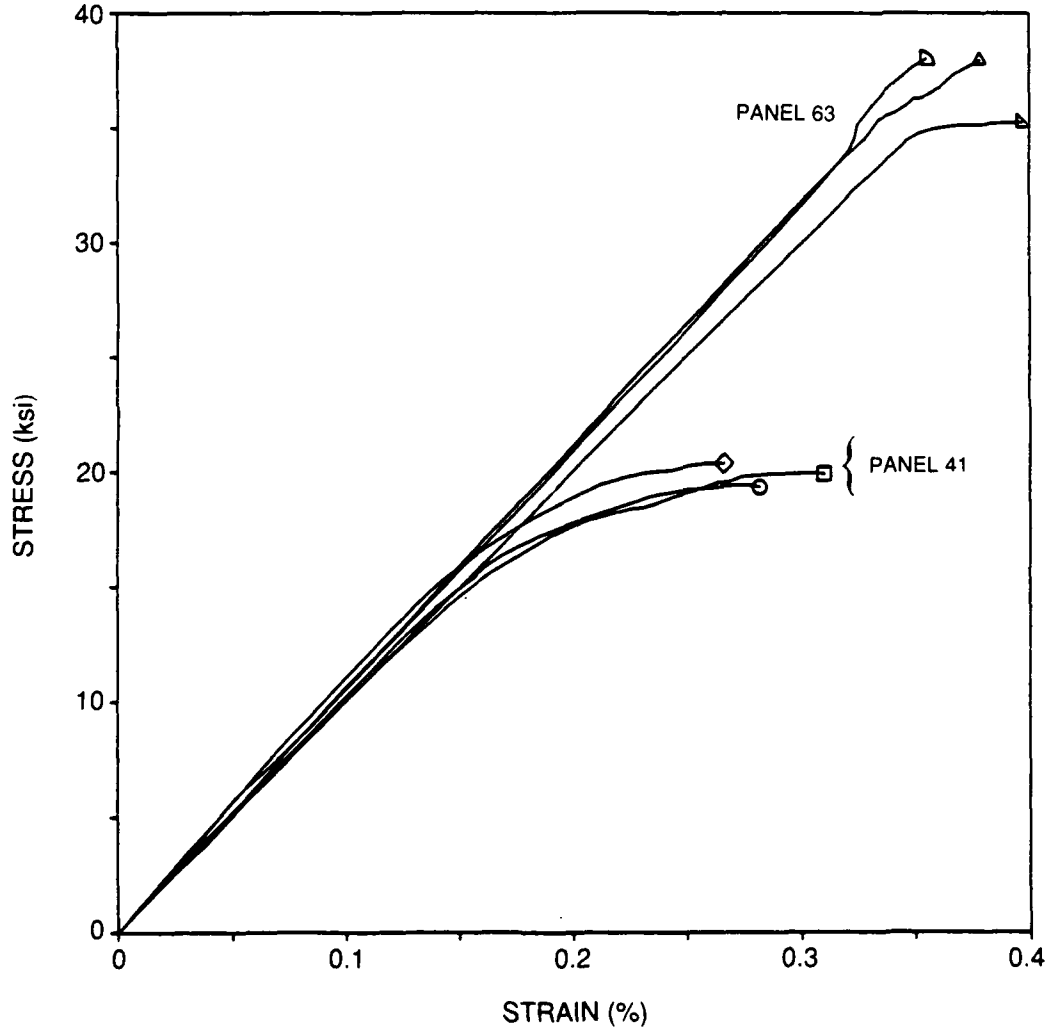

Figure 12. Compressive response at 20°C for 2D carbon fiber reinforced CMC derived from polysilazane/methylvinyisilane reimpregnation.

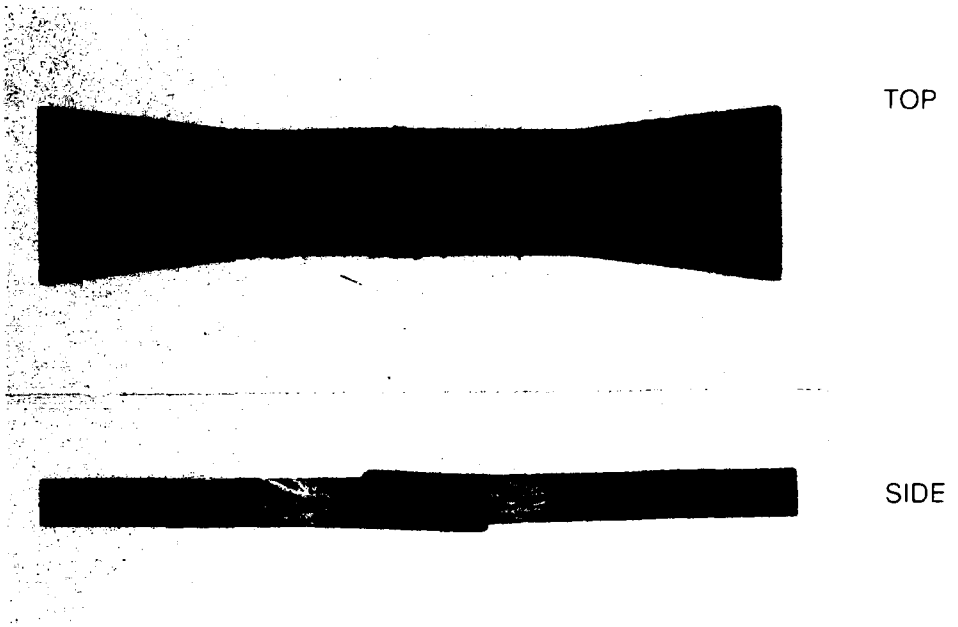

(a) PANEL 10195-41

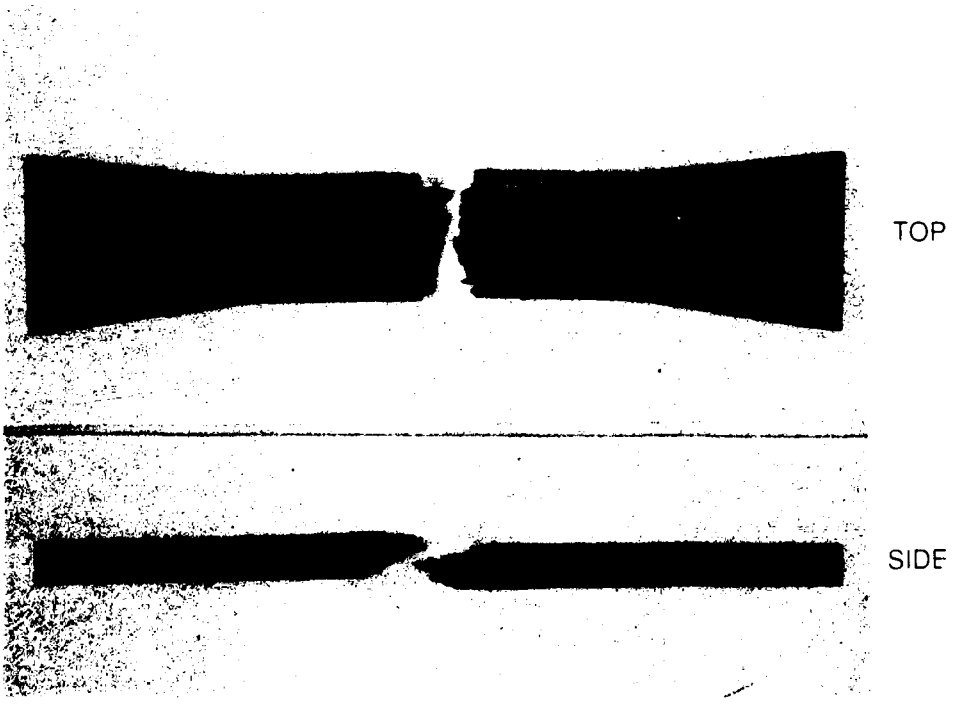

(b) PANEL 10195-63

Figure 13. Comparison of compressive failure mode.

91-1-4-6

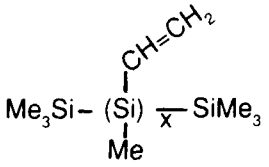

Figure 14a. Structure of SiH free methylvinylsilane (Y-12044 NH).

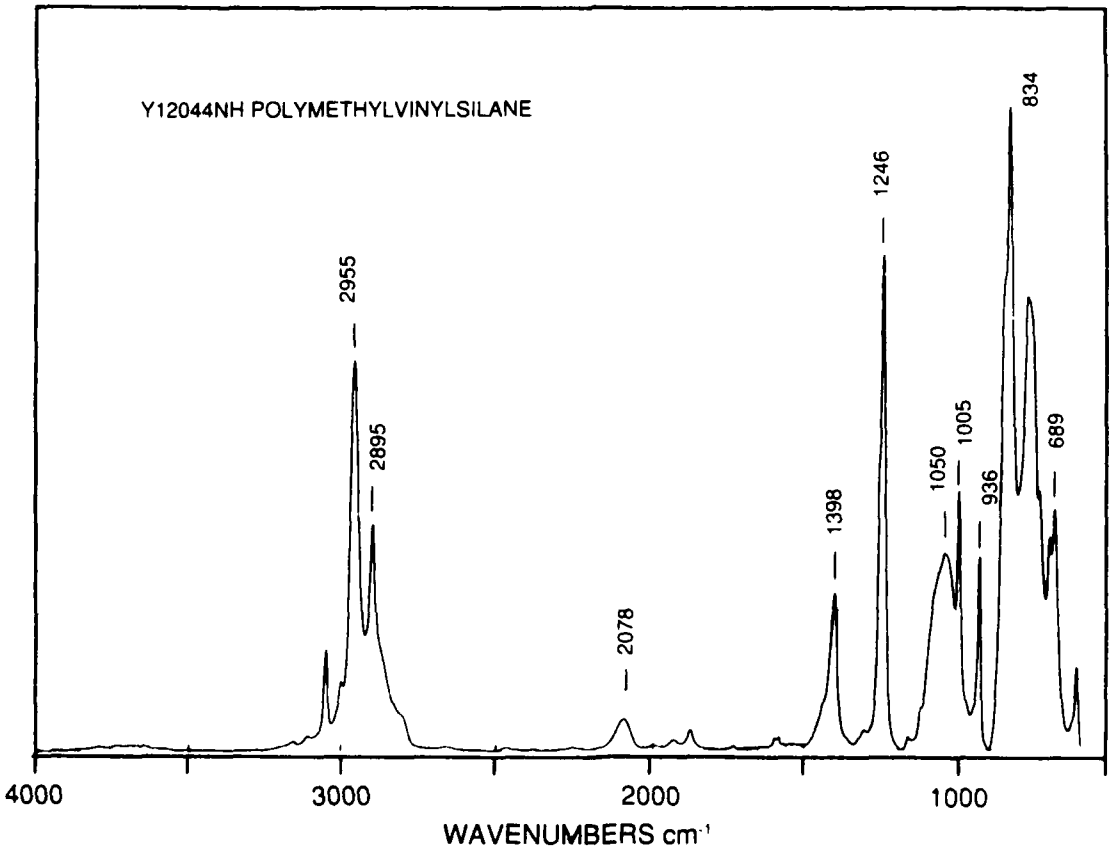

Figure 14b. FTIR spectrum of Y-12044 NH methylvinyisilane.

90-6-33-7

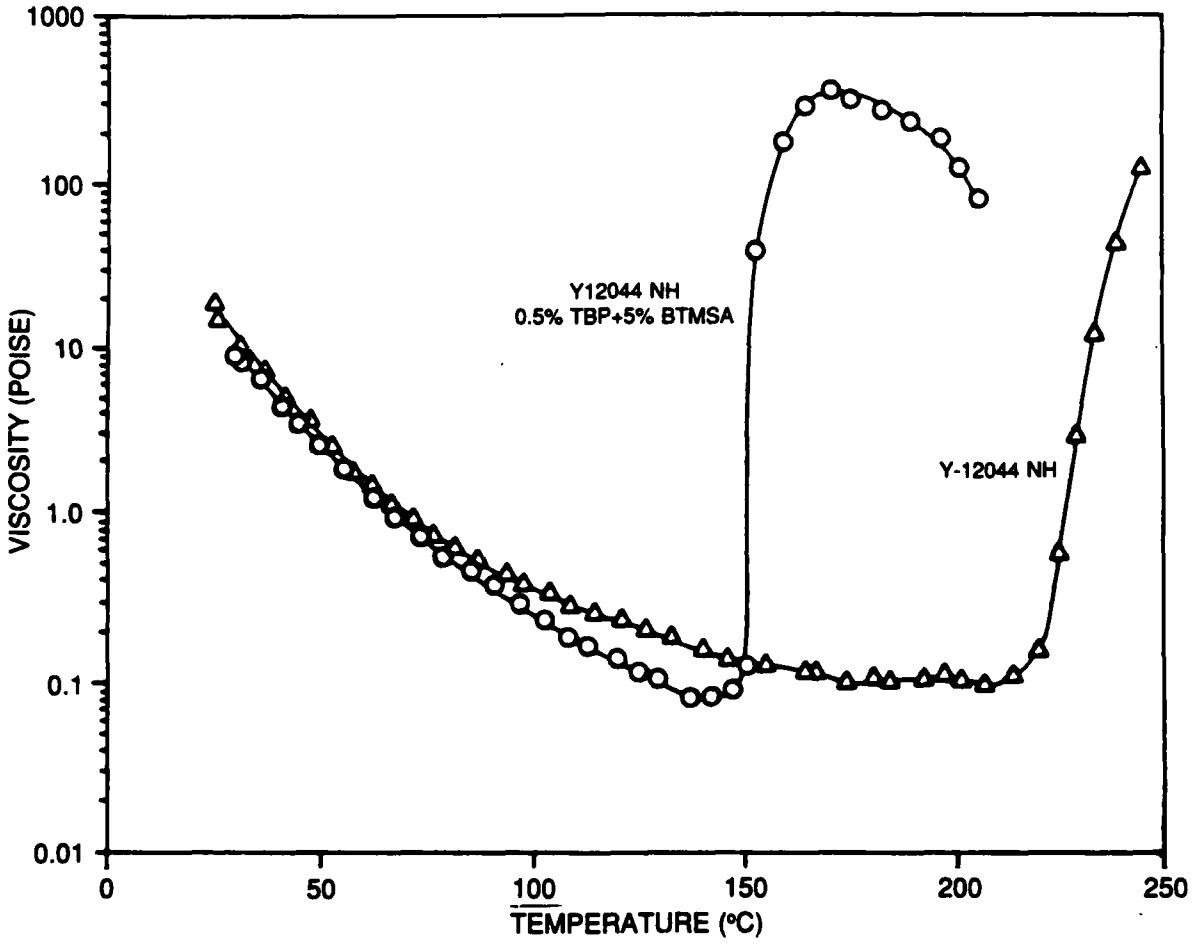

Figure 15. Use of initiators (TBP) and accelerant, (BTMSA) to lower cure temperature of SiH free vinylmethylsilane (Y12044NH).

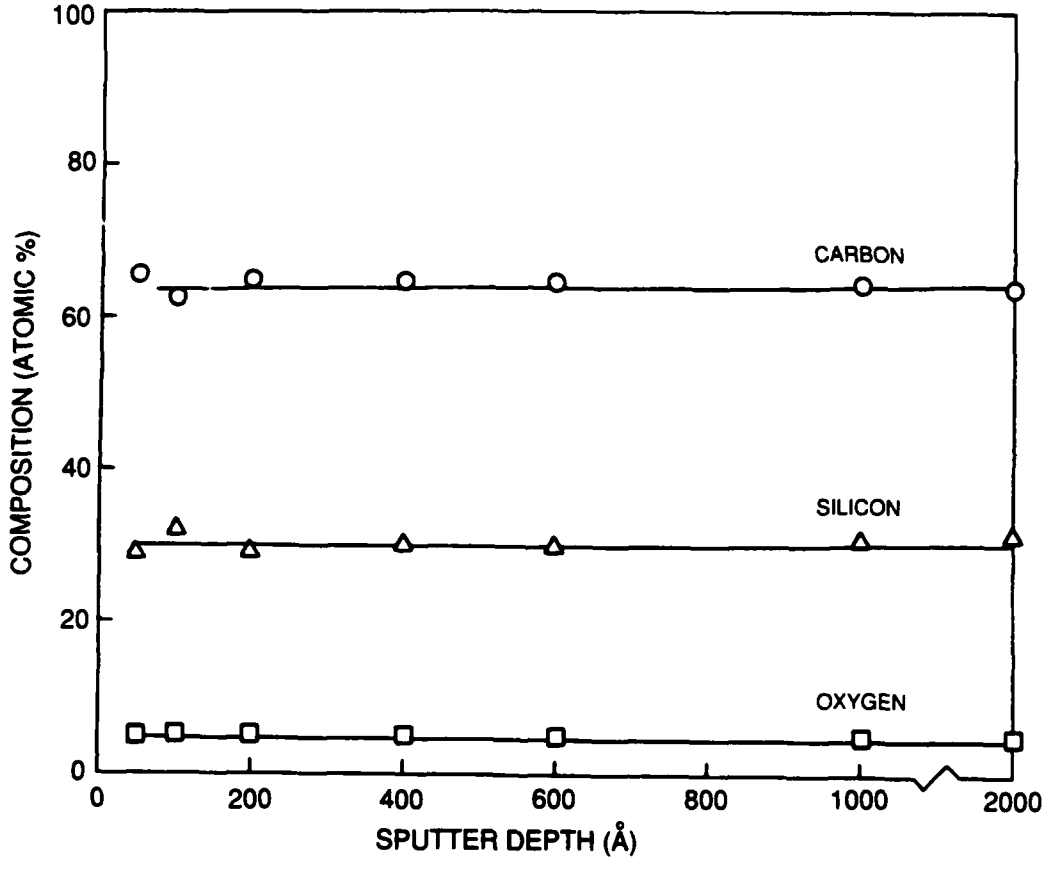

Figure 16. Auger analysis of fracture surface of Y-12044 NH derived 800°C pyrolysis product.

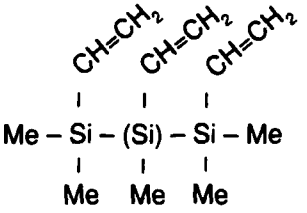

Figure 17a. Structure of W1-164.

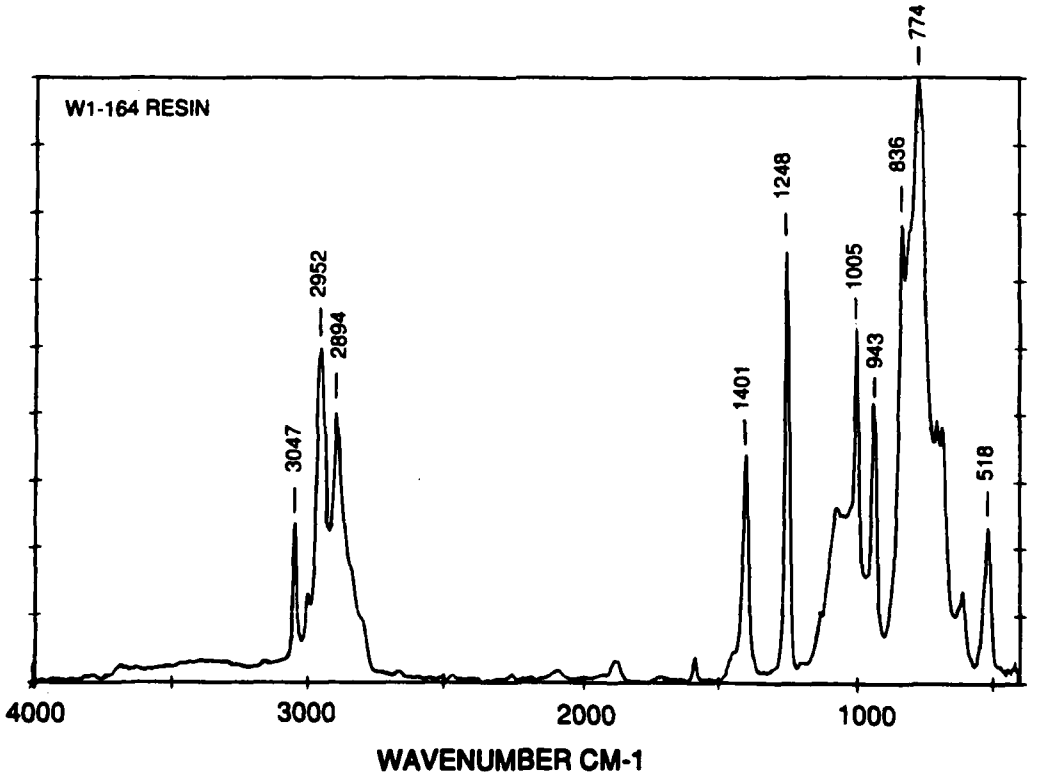

Figure 17b. FTIR spectrum of W1-164 vinyl endblocked polymethylvinylsilane.

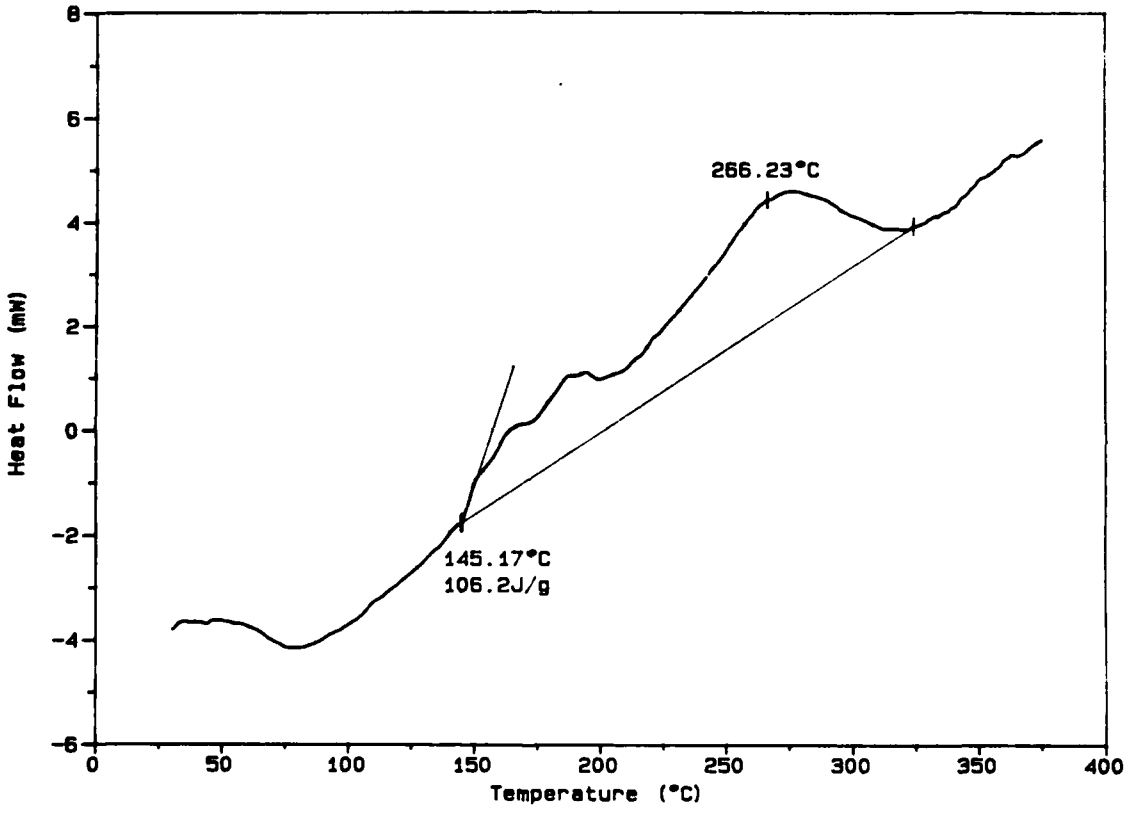

Figure 18. Heat flow as a function of temperature in nitrogen atmosphere for W1-164 polymer.

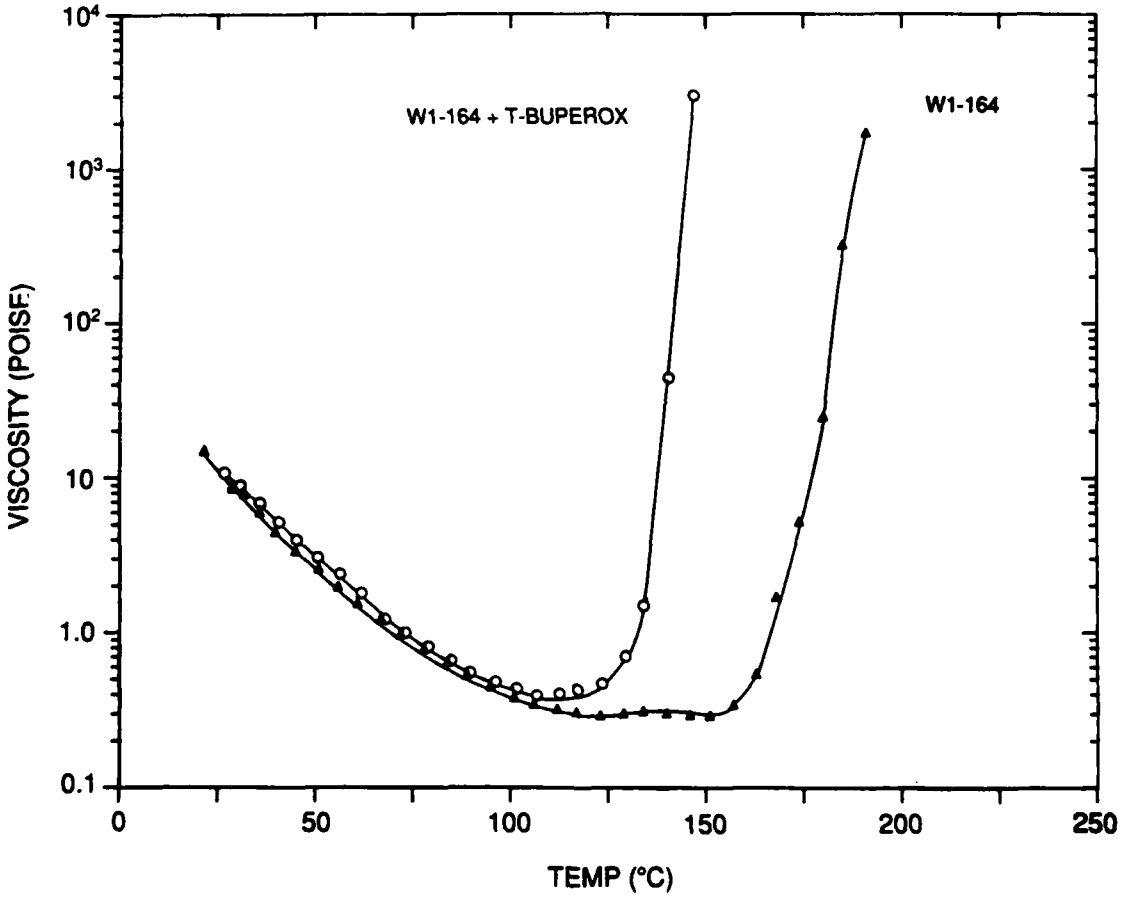

Figure 19. Curing characteristics of W1-164 as indicated by viscosity change.

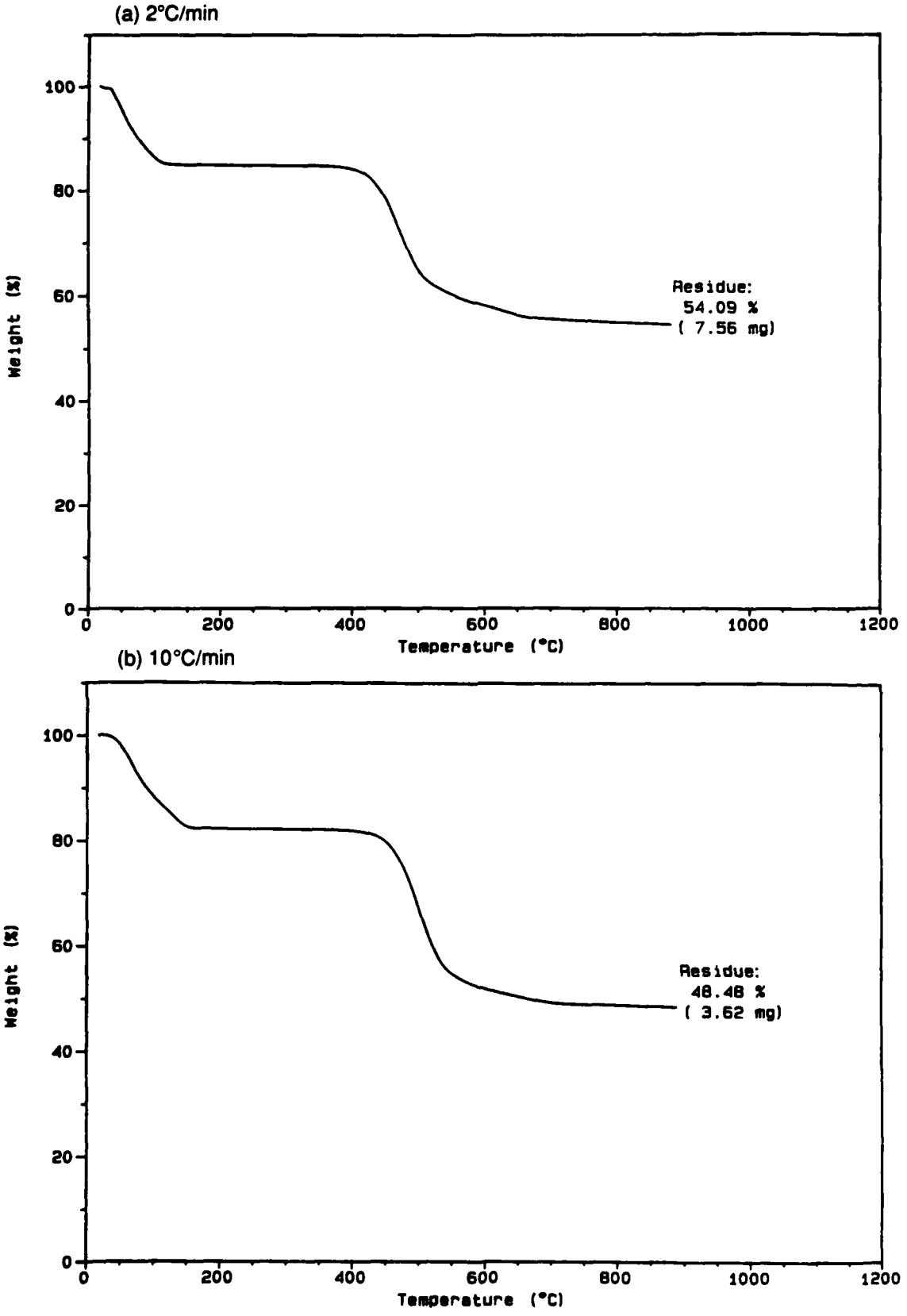

Figure 20. Thermogravimetric data for W1-164 as a function of heating rate in nitrogen atmosphere.

91-1-4-10

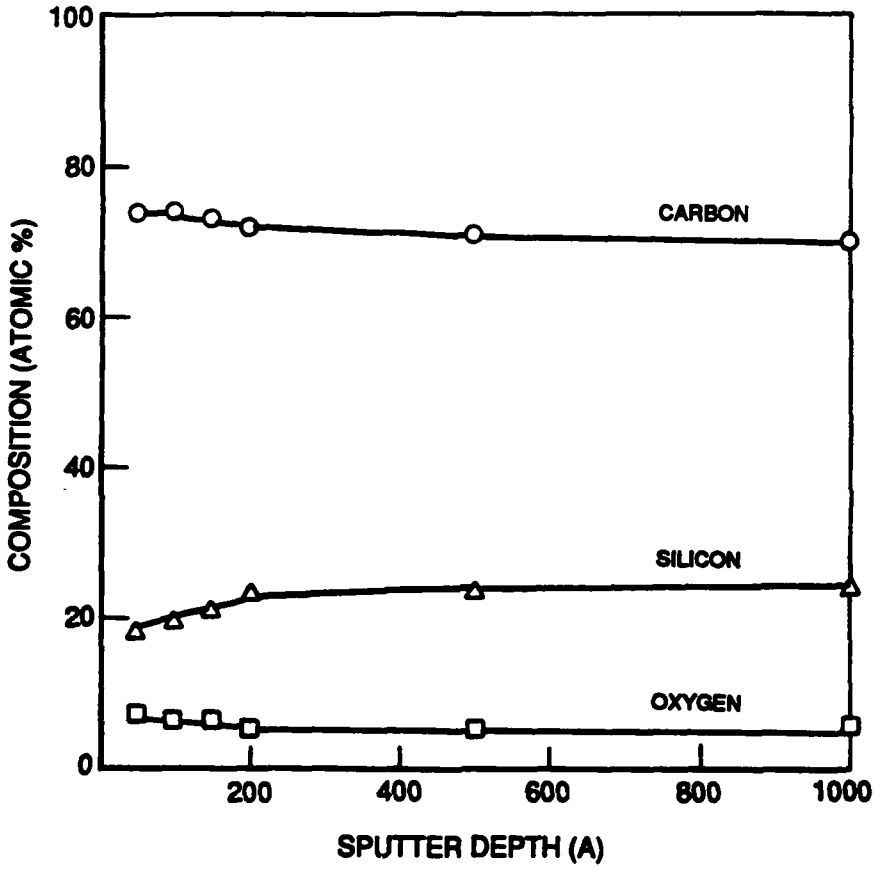

Figure 21. Auger analysis of fracture surface from W1-164 derived 850°C pyrolysis product.

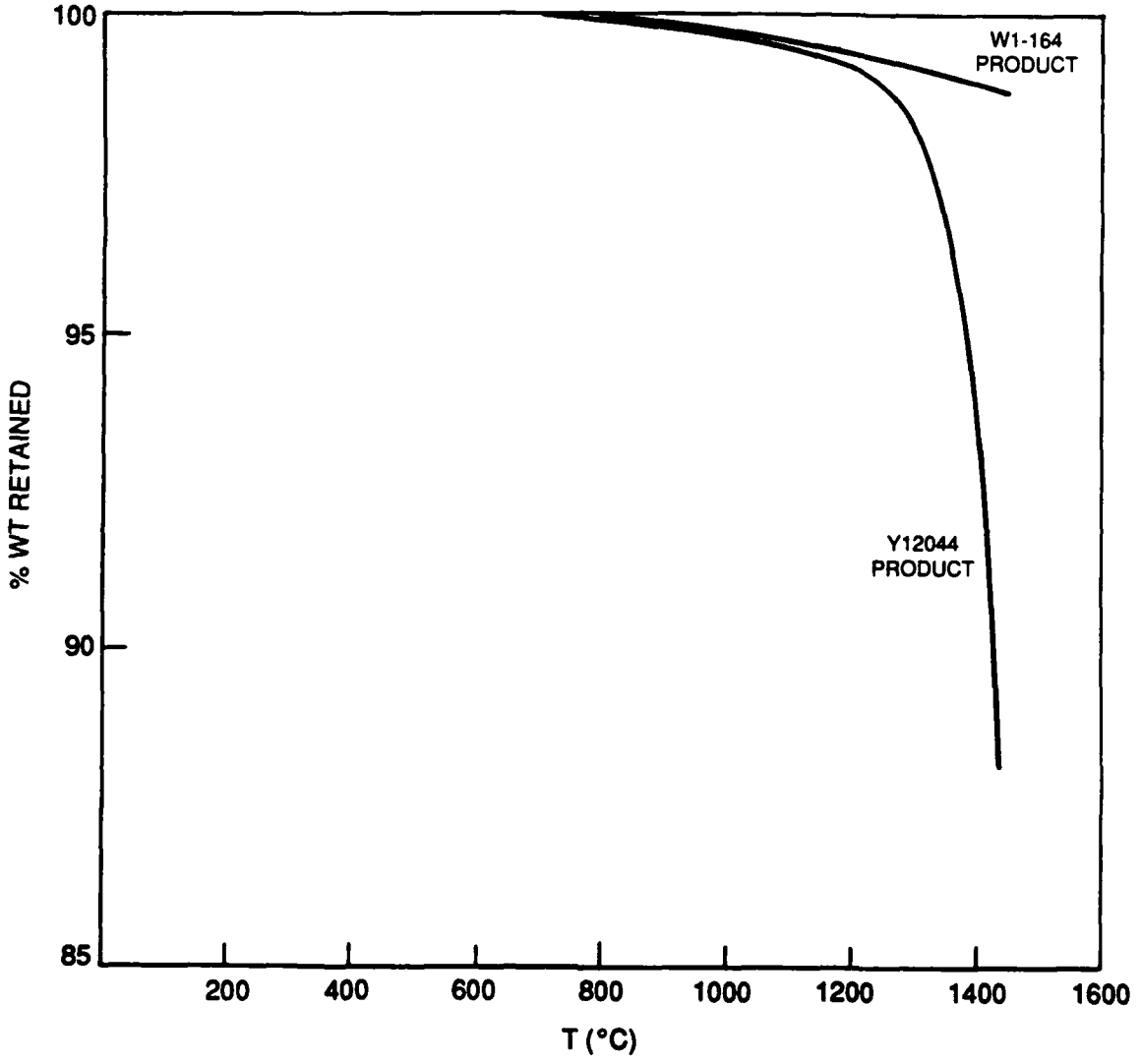

Figure 22. Converted ceramic stability on heating to 1440°C at 2°C/min.

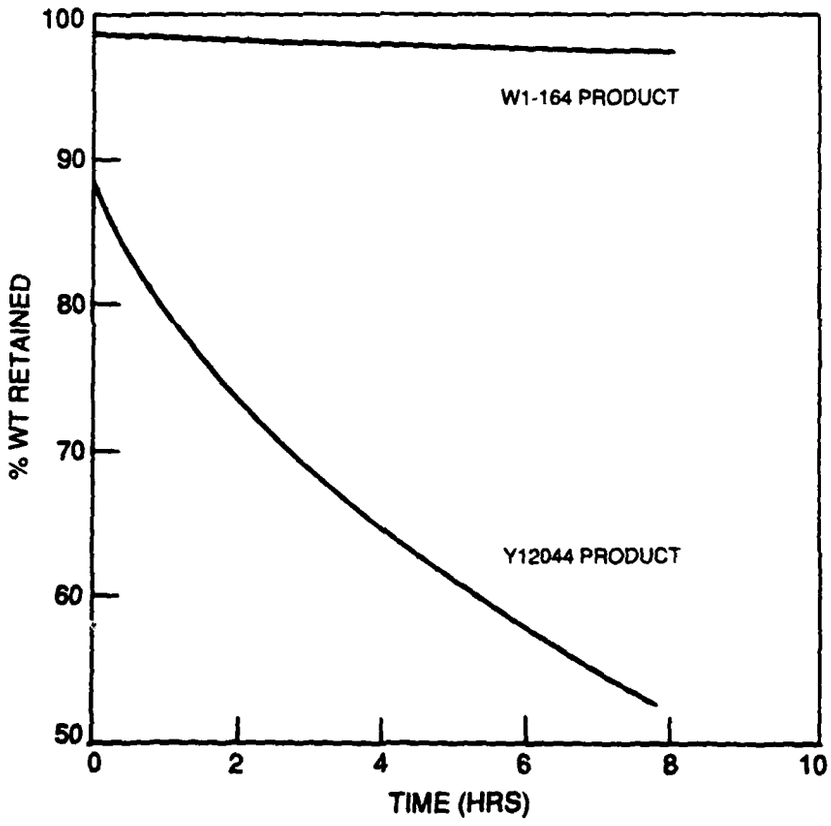

Figure 23. Converted ceramic stability during isothermal hold at 1440°C.

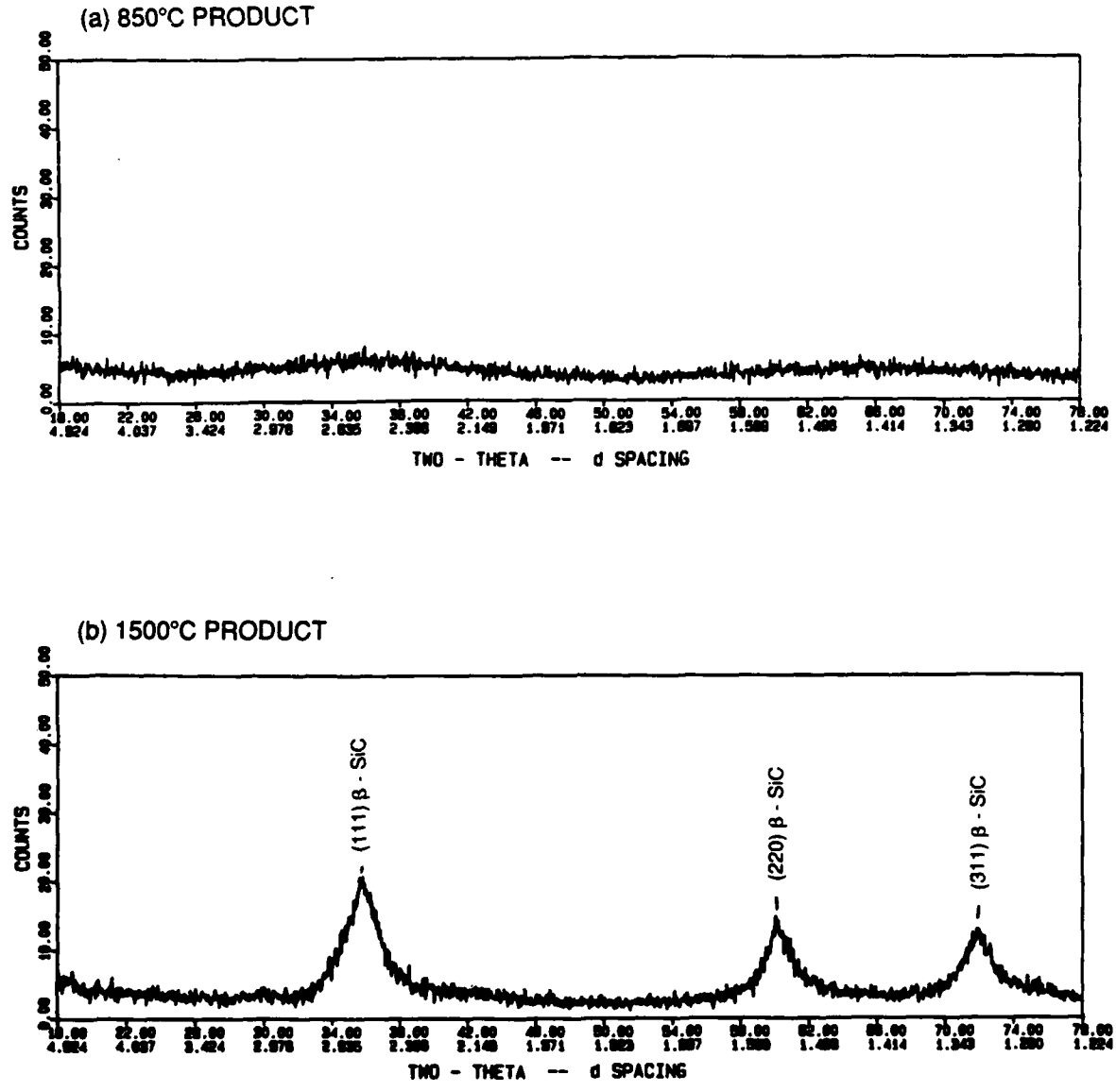

Figure 24. XRD analysis of pyrolyzed ceramics from W1-164 polymethylvinylsilane.

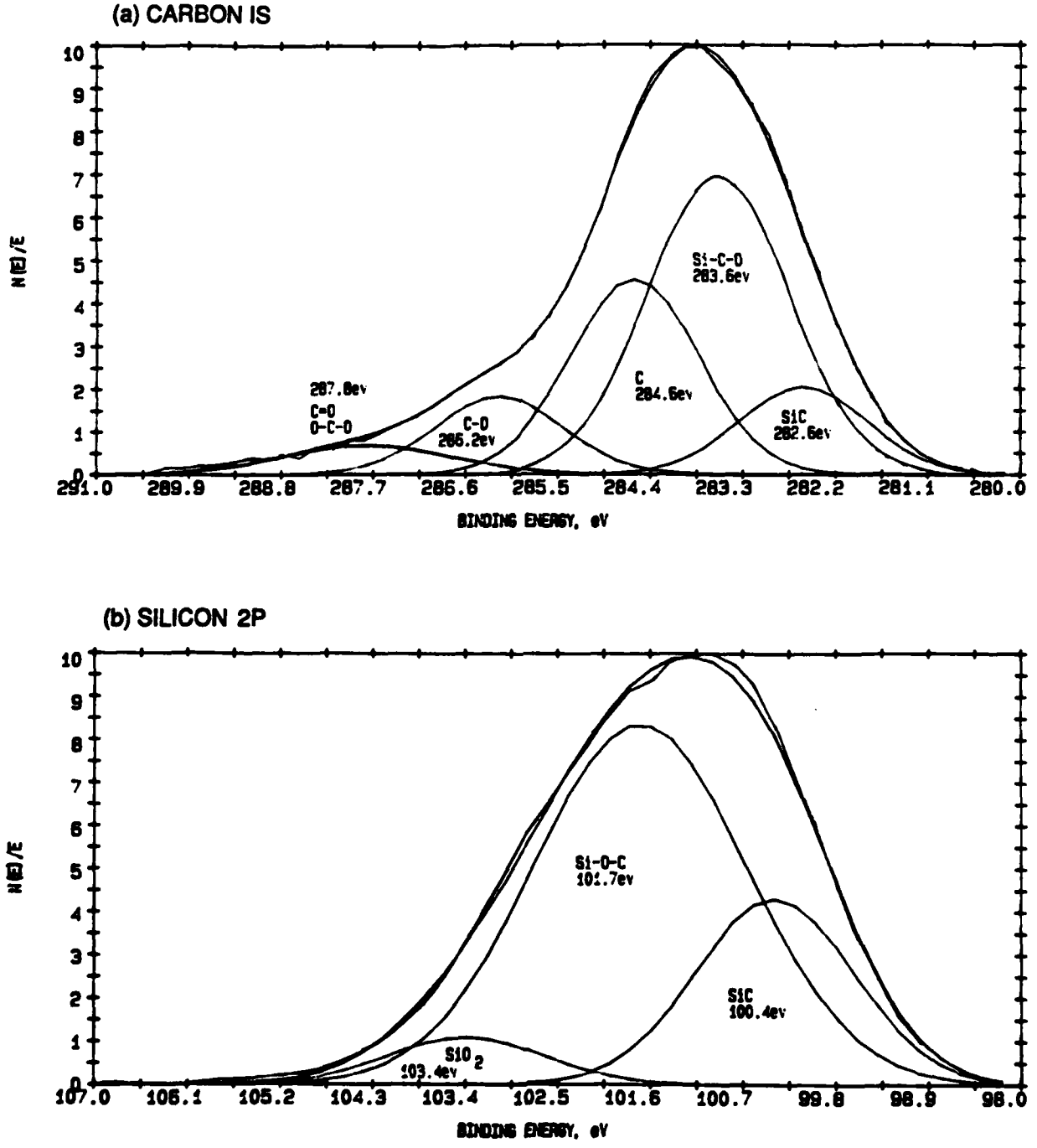

Figure 25. Curve-fit analysis of carbon 1s and silicon 2p peaks from XPS survey of Y-12044 product converted at 900°C.

(a) CARBON IS

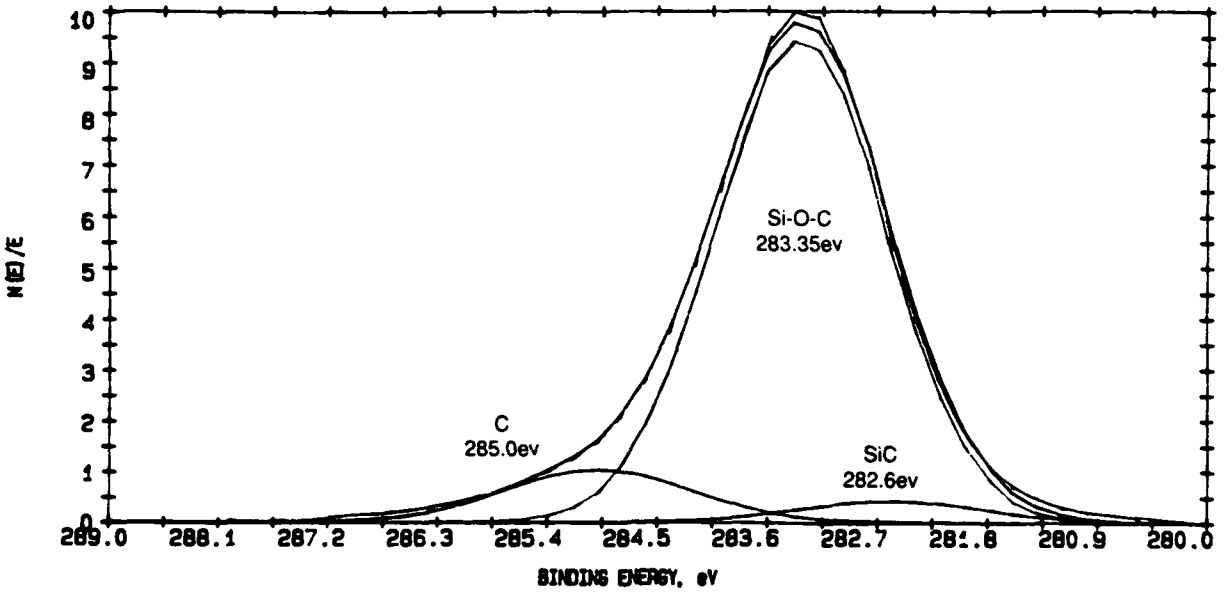

(b) SILICON 2P

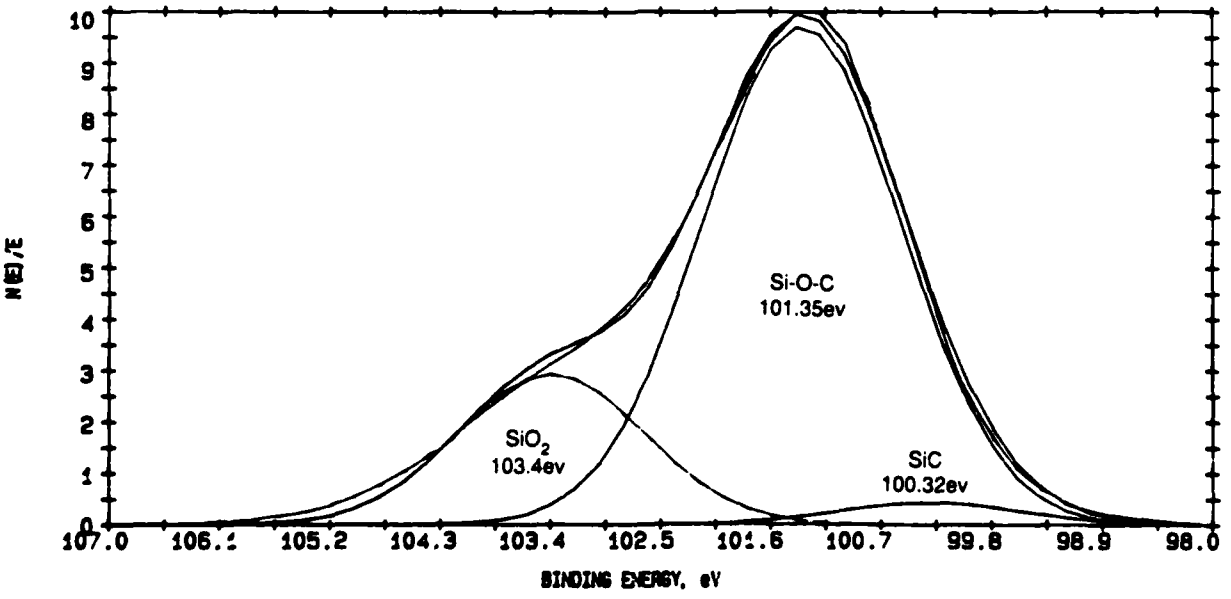

Figure 26. Curve-fit analysis of carbon 1s and silicon 2p peaks from XPS survey of Y-12044 product converted at 1500°C.

90-1-4-16

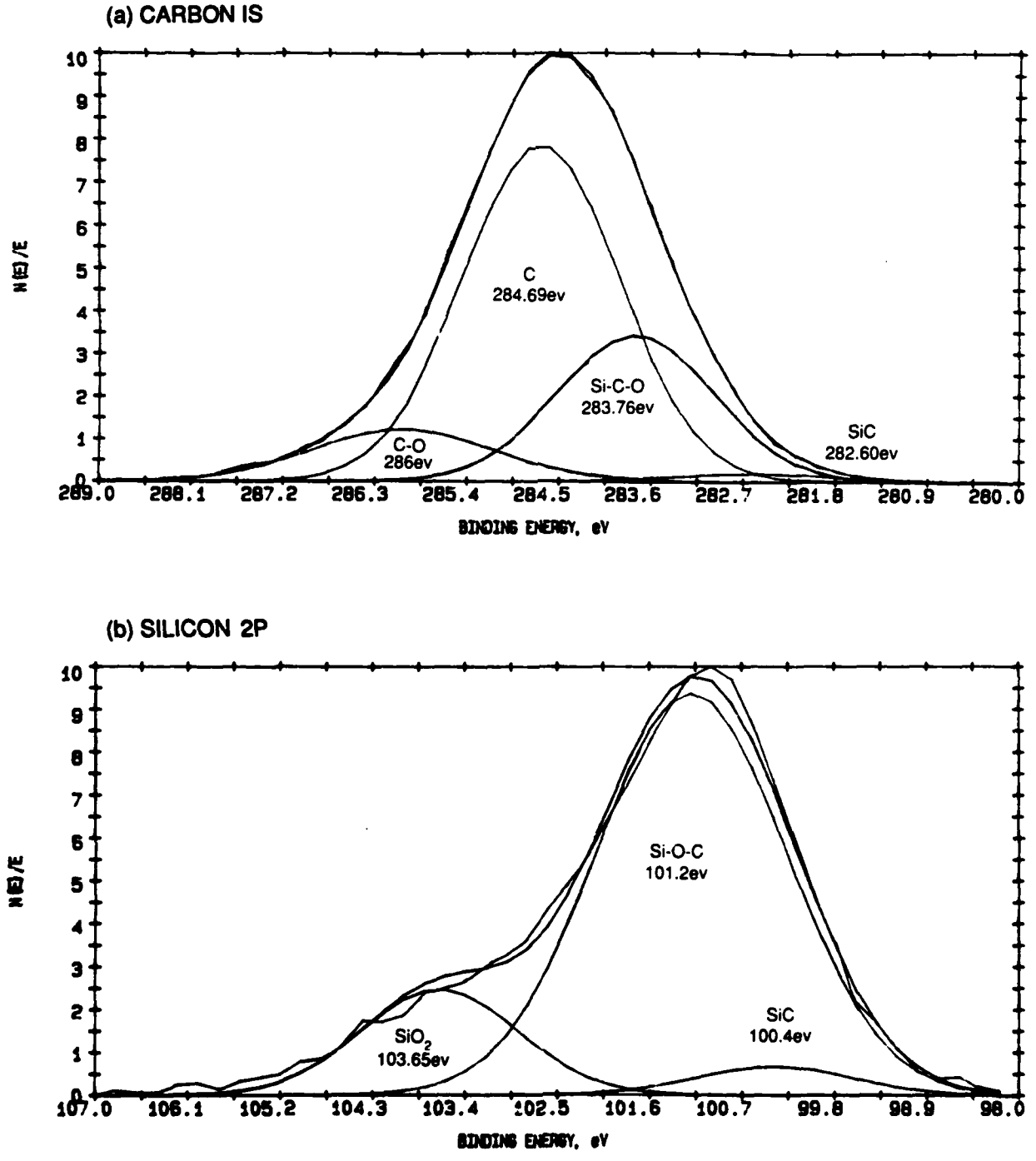

Figure 27. Curve-fit analysis of carbon 1s and silicon 2p peaks from XPS survey of W1-164 product converted at 850°C.